Supplementary Information - Impacts of irrigation expansion on moist-heat stress based on IRRMIP results

Yao et al.

Contents

List of Tables **3**

List of Figures **4**

1 Supplementary Notes **6**

1.1 Supplementary Note 1: Participating ESMs and their irrigation implementation 6

1.2 Supplementary Note 2: IRRMIP simulation protocol 9

1.3 Supplementary Note 3: Other moist-heat metrics 9

2 Supplementary Figures **12**

2.1 Supplementary Figures 1: Appendix Figures 12

2.2 Supplementary Figures 2: Results of individual ESMs 22

2.3 Supplementary Figures 3: Results of individual metrics 33

Supplementary References **48**

List of Tables

S1 Simulation protocol of IRRMIP 10
S2 Details of ESMs outputs 10

List of Figures

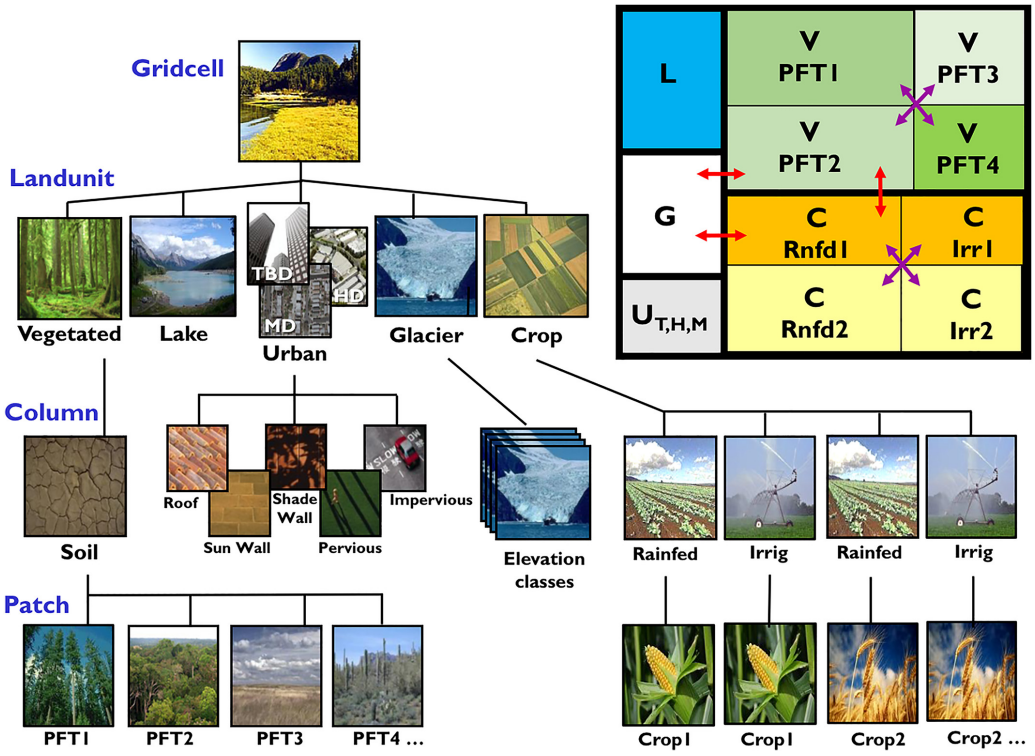
S1 Sub-grid cell structure of the Community Land Model 5 . . . 6
S2 Irrigation scheme used in IPSL-CM6 . . . 8
S3 Irrigated fraction in different years, and simulated irrigation water withdrwal during different periods without irrigation expansion . . . 12
S4 Impacts of different forcings on various extreme events of 2-meter air temperature 13
S5 Impacts of different forcings on various extreme events of HUMIDEX . . . 14
S6 Impacts of different forcings on various extreme events of wet-bulb temperature 14
S7 Changes in the frequency of extreme events of other metrics induced by irrigation expansion . . . 15
S8 Time series of exposure hours to 2-meter air temperature extremes over four groups of grid cells . . . 16
S9 Multi-year mean monthly irrigation water withdrawal . . . 17
S10 Multi-year mean monthly maximum 2-meter air temperature . . . 18
S11 Multi-year mean monthly maximum HUMIDEX . . . 19
S12 Multi-year mean monthly maximum wet-bulb temperature . . . 20
S13 Irrigation-expansion induced impacts on mean and extreme 2-meter air temperature . . . 20
S14 Irrigation-expansion induced impacts on mean and extreme specific humidity . . 21
S15 Simulated irrigation water withdrawal of individual models . . . 22
S16 Impacts of different forcings on absolute values of 2-meter air temperature, HUMIDEX, and wet-bulb temperature extreme event (CESM2) . . . 23
S17 Impacts of different forcings on absolute values of 2-meter air temperature, HUMIDEX, and wet-bulb temperature extreme event (CESM2_gw) . . . 24
S18 Impacts of different forcings on absolute values of 2-meter air temperature, HUMIDEX, and wet-bulb temperature extreme event (NorESM2) . . . 25
S19 Impacts of different forcings on absolute values of 2-meter air temperature, HUMIDEX, and wet-bulb temperature extreme event (E3SMv2) . . . 26
S20 Impacts of different forcings on absolute values of 2-meter air temperature, HUMIDEX, and wet-bulb temperature extreme event (IPSL-CM6) . . . 27
S21 Impacts of different forcings on absolute values of 2-meter air temperature, HUMIDEX, and wet-bulb temperature extreme event (CNRM-CM6-1) . . . 28
S22 Impacts of different forcings on frequency of 2-meter air temperature, HUMIDEX, and wet-bulb temperature extreme event (CESM2) . . . 29
S23 Impacts of different forcings on frequency of 2-meter air temperature, HUMIDEX, and wet-bulb temperature extreme event (CESM2_gw) . . . 30
S24 Impacts of different forcings on frequency of 2-meter air temperature, HUMIDEX, and wet-bulb temperature extreme event (NorESM2) . . . 30
S25 Impacts of different forcings on frequency of 2-meter air temperature, HUMIDEX, and wet-bulb temperature extreme event (E3SMv2) . . . 31

S26 Impacts of different forcings on frequency of 2-meter air temperature, HUMIDEX, and wet-bulb temperature extreme event (IPSL-CM6) . . . 31
S27 Impacts of different forcings on frequency of 2-meter air temperature, HUMIDEX, and wet-bulb temperature extreme event (CNRM-CM6-1) . . . 32
S28 Impacts of different forcings on absolute values of various extreme events of 2-meter air temperature . . . 33
S29 Impacts of different forcings on absolute values of various extreme events of HUMIDEX . . . 34
S30 Impacts of different forcings on absolute values of various extreme events of wet-bulb temperature . . . 35
S31 Impacts of different forcings on absolute values of various extreme events of Apparent Temperature . . . 36
S32 Impacts of different forcings on absolute values of various extreme events of Discomfort Index . . . 37
S33 Impacts of different forcings on absolute values of various extreme events of Temperature Humidity Index for Comfort . . . 38
S34 Impacts of different forcings on absolute values of various extreme events of Temperature Humidity Index for Physiology . . . 39
S35 Impacts of different forcings on absolute values of various extreme events of the temperature with 65% of the swamp coolers . . . 40
S36 Impacts of different forcings on absolute values of various extreme events of the temperature with 80% of the swamp coolers . . . 41
S37 Impacts of different forcings on frequency of various extreme events of Discomfort Index . . . 42
S38 Impacts of different forcings on frequency of various extreme events of Apparent Temperature . . . 43
S39 Impacts of different forcings on frequency of various extreme events of Temperature Humidity Index for Comfort . . . 43
S40 Impacts of different forcings on frequency of various extreme events of Temperature Humidity Index for Physiology . . . 44
S41 Impacts of different forcings on frequency of various extreme events of the temperature with 65% of the swamp coolers . . . 44
S42 Impacts of different forcings on frequency of various extreme events of the temperature with 80% of the swamp coolers . . . 45
S43 Annual hours exposed to HUMIDEX extreme events over grid cells with different extent of irrigation expansion . . . 46
S44 Annual hours exposed to wet-bulb temperature extreme events over grid cells with different extent of irrigation expansion . . . 47

1 Supplementary Notes

1.1 Supplementary Note 1: Participating ESMs and their irrigation implementation

The Community Earth System Model version 2 (CESM2), is a state-of-art Earth system model, with the Community Atmosphere Model version 6 (CAM6)[2] as the atmosphere model, the Community Land Model version 5 (CLM5) as the land model, and the Model for Scale Adaptive River Transport (MOSART) as the routing model[3–6]. The CLM5 is forced by atmospheric variables from the CAM6 (in coupled simulations), or from external datasets (in off-line simulations), to simulate the biophysical and biochemical processes in the land system. A sub-grid cell level structure is used in CLM5, according to which a grid cell is formed by five land cover types: natural vegetation, lake, urban, glacier, and cropland, and all these land cover types are further divided into multiple soil columns and patches (Figure S1). The calculations of hydrological, energy, and carbon fluxes are operated individually over each column or patch, then weighted averaged to generate the grid cell level outputs, which then are exchanged with CAM6 and MOSART.



Supplementary Figure S1 | Sub-grid cell structure of the Community Land Model 5 (CLM5) land datasets. Figure from the description paper of CLM5.[3]

Under the cropland cover type, 31 different crops are implemented, which are then merged into 8 active crop functional types due to the lack of parameterisation of some crops. For each crop functional type, two patches are used, representing irrigated and rainfed cropland, respectively. Over each irrigated cropland patch, every day at 6:00 AM local time, the model checks (i) whether the crop LAI is more than 0, and (ii) whether the actual soil moisture (SM_{actual}) is

less than the threshold (SM_{thresh}). If both conditions are satisfied, the model activates the irrigation, and the amount of water used for irrigation (IW) is calculated as the deficit between SM_{actual} and the target soil moisture (SM_{target}). Then, the water is applied as the rainfall under the canopy evenly during a period of 4 hours, namely 6:00 AM to 10:00 AM local time. The water used for irrigation is abstracted from the surface water in the main channel in MOSART, and when the available surface water is not sufficient, ocean water will be withdrawn to close the water balance. CLM5 also provide options for limiting water withdrawal and groundwater use for irrigation, which are not used in this study. A study applied over the Pacific Northwest watershed shows that CLM5 with this irrigation module generally well simulated the water, energy, carbon fluxes and crop phenology[7], but at the global level, this module substantially underestimate the irrigation water withdrawal[8].

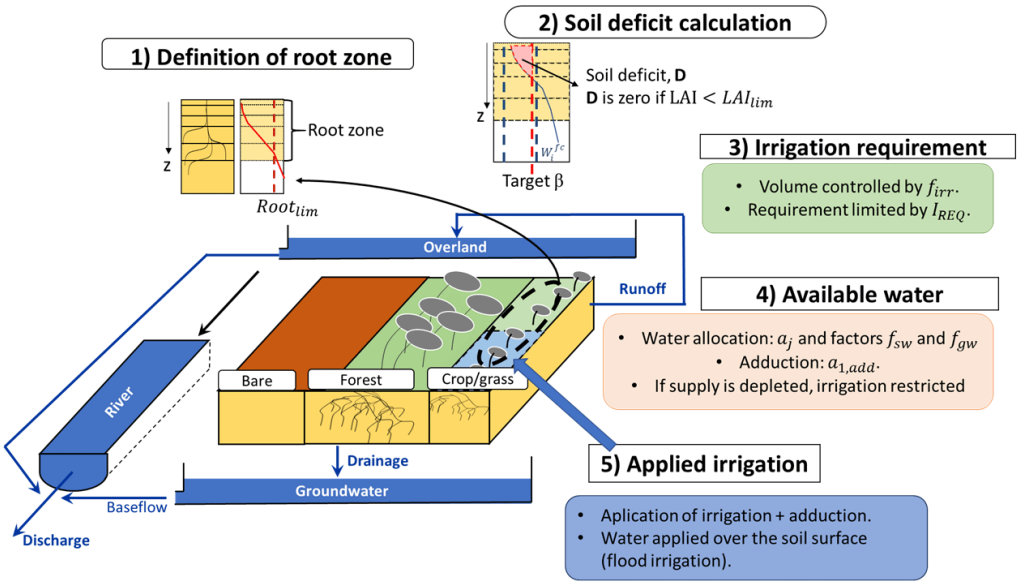
The difference between CESM2 and CESM2_gw is in CESM2_gw, an intercell lateral groundwater interaction and an aquifer pumping process are implemented[9]. When the water in the main channel cannot satisfy the irrigation water demand in the gridcell, groundwater withdrawal will be activated, with the groundwater in the soil layers firstly pumped and aquifer later. The groundwater pumping of a gridcell is assumed to be operated over a single well, and cause a decrease in groundwater table, which then pertubates the baseflow interactions with neighbouring gridcells. Evaluation results indicate that this newly added feature greatly improved the model's ability to reproduce the spatiotemperal groundwater-level changes over the US high Plains and Central valley Aquifer.

The Norwegian Earth System Model (NorESM)[10] shares the same atmosphere (CAM6) and land system model (CLM5) with CESM2, except for some additional developments like new chemistry/aerosol/cloud module (OsloAero6[11]) and improved conservation of energy and angular momentum[12].

The Energy Exascale Earth System Model (E3SMv0) was developed based on CESM1, with CAM5, CLM4.5, MOSART, and POP as the atmosphere, land, river routing, and ocean model[13]. In developing E3SMv1, the ocean model was replaced by MPAS-O, and many new model features were added to each component model, which resulted in the E3SM Land Model (ELM), the E3SM Atmosphere Model (EAM) and the routing model (MOSART-Water Management: MOSART-WM), so E3SMv1 differs quite significantly from CESM1 and CESM2[14,15]. The key changes in E3SM's irrigation module compared to that in CLM4.5 are (i) a two-way coupling between ELM and MOSART-WM, which constrains surface water withdrawal based on water availability[16]; and (ii) the introduction of a fraction (F_{grd}) that determines how much irrigation water is derived from the groundwater, which is estimated from water use statistics[16,17]. In ELM, the need for irrigation is also checked at 6:00 am local time, and the demand is then partitioned into two parts, groundwater demand and surface water demand, based on F_{grd}. The groundwater demand is always satisfied, but the surface water demand is evaluated by

MOSART-WM to decide how much surface water is supplied based on the water management rules. Compared to the one-way coupling scheme used in CLM4.5, this new scheme shows some advantages in more realistically simulating groundwater level and irrigation water-use seasonal pattern[16].

The Institut Pierre-Simon Laplace Climate Model version 6 (IPSL-CM6[19]) uses LMDZ6 as the atmosphere model[18] and the Organising Carbon and Hydrology in Dynamic Ecosystems version 2.2 (ORCHIDEE 2.2) as the land model, here with a new irrigation module[20]. As shown in Figure S2, a soil moisture deficit is calculated by confronting the actual soil moisture in the root zone to a target soil moisture above which irrigation is not needed. The deficit is calculated for the soil column of gathering cropland and grassland, whether irrigated or not, as irrigated cropland and grassland are not treated apart. The irrigation demand, however, is obtained by multiplying the soil moisture deficit by the fraction of irrigated land. Three sources of water, from the stream, overland, and (renewable) groundwater reservoirs, are considered to supply the demand, all of them with a limitation on water withdrawal for ecological protection. The share of withdrawals between surface water (stream and overland) and groundwater is given in each grid cell by the fractional areas equipped for surface and groundwater irrigation from a global map[21], and the amount of water from the two surface sources is proportional to their available water. The withdrawn water is applied at the soil surface over the whole crop and grass column, and a maximum irrigation rate is set in the model to prevent from excessive surface runoff unrealistic irrigation application.



Supplementary Figure S2 | Irrigation scheme used in IPSL-CM6. Figure from the description paper of this scheme.[20]

In this study, the climate model used by the French National Center for Meteorological Research (CNRM) is an upgraded version of the CNRM-CM6-1 climate model[32]. It is based on the ARPEGE-Climat v6.3 atmospheric general circulation model[33], and the SURFEX v8.0 surface modeling platform[34] to simulate ocean and lake fluxes, as well as land surface pro-

cesses. These land surface processes are simulated using the ISBA-CTRIP (Interaction-Soil-Biosphere-Atmosphere - CNRM version of the Total Runoff Integrating Pathways; `https://www.umr-cnrm.fr/spip.php?article1092&lang=en`) land surface model that provides a physical and realistic representation of the continental hydrology[35], as well as a simple but complete representation of the land surface carbon cycle and of the land use land cover changes that affect energy, water, and carbon exchanges[36]. Irrigation water withdrawals have recently been introduced into ISBA-CTRIP[37]. Irrigation water demand is imposed as an external forcing, preferentially in the cropland portion of each model grid cell. The irrigation water flux is then partitioned between flood, sprinkler, and drip irrigation, and withdrawn from groundwater reservoirs and conceptual small dams to close the global water budget. In this study, the irrigation water demands are from a global reconstructed hydrological dataset based on simulations[22].

1.2 Supplementary Note 2: IRRMIP simulation protocol

The configurations of simulations should be the same as in the AMIP experiment[23] of CMIP6, which means that only atmospheric and land models are activated. Sea surface temperatures and sea ice concentrations are prescribed consistent with observations. Other forcings, including land use, land cover, volcanic aerosols, solar variability, greenhouse gas concentrations and anthropogenic aerosols, are transient and prescribed from historical data. We recommend using the LUH2 transient irrigation extent data[24], but alternative data sources could be used. The simulation period is from 1^{st} January 1901 to 31 December 2015. The experiment consists of two ensembles, and for every ensemble, at least 3 members are recommended. Modelling teams are free to choose their own spatial resolution and model settings. This study uses the results from six ESMs, varying in spatial and temporal resolution and number of ensemble members. More details are in Table S2.

1.3 Supplementary Note 3: Other moist-heat metrics

Apparent temperature (AT) is a "feel-like" temperature perceived by human bodies, considering the impacts of temperature, radiation, humidity, and wind speed[25]. The AT used in this study ignores the impact of sunlight to detect the thermal comfort of an adult walking outdoors in the shade[26]. AT is calculated as

$$\mathrm{AT} = T_{\mathrm{C}} + \frac{3.3 e_{\mathrm{RH}}}{1000} - 0.7 u_{10\ \mathrm{m}} - 4, \tag{S1}$$

where u_{10m} is the wind speed at 10-meter height (m s^{-1}), T_C is the temperature at 2-meter height (°C), e_{RH} (Pa) is the vapour pressure calculated based on relative humidity (RH) and saturated vapour pressure (e_s in Pa):

$$e_{\mathrm{RH}} = \mathrm{RH} e_{\mathrm{s}}, \tag{S2}$$

Table S1: Simulation protocol of IRRMIP

Experiment ID	Description	Notes
tranirr	Transient irrigation extent	For models in which transient irrigation extent is not possible, prescribed present-day irrigation extent can be used as an alternative
1901irr	Irrigation extent kept constant at 1901 level	For models which apply irrigation flux as a forcing, the flux should be kept constant at 1901 levels. For models whose implementation of irrigation is parameterised in the source code, the input land cover data should be modified to keep the area equipped for irrigation constant throughout the simulation.

Table S2: Details of ESMs outputs

ESMs	Spatial resolution	Output frequency	Ensemble members
CESM2	0.9°x 1.25°	3 hour	3
CESM2gw	0.9°x 1.25°	3 hour	3
NorESM	0.9°x 1.25°	3 hour	3
E3SM	0.5°x 0.5°	3 hour	2
IPSL-CM6	0.5°x 0.5°	3 hour	1
CNRM-CM6-1	1.4°x 1.4°	daily	5

AT prediction is provided by the Australian Bureau of Meteorology and the National Weather Service of the United States.

The Temperature Humidity Index for Comfort (THIC) is also a comfort algorithm used for quantifying livestock's comfort[27]. The original calibration is specifically used for pigs, which is calculated as follows:

$$\mathrm{THIC} = 0.72T_{\mathrm{w}} + 0.72T_{\mathrm{C}} + 40.6 \tag{S3}$$

where T_w is the wet bulb temperature (°C).
Considering that it is not easy to approach the maximum cooling impacts, another two metrics, T_{s65} and T_{s80}, in which 65 % or 80 % of the swamp coolers are approached, respectively, are developed.

$$T_{\mathrm{s}} = T_{\mathrm{C}} - \frac{\eta}{100}\left(T_{\mathrm{C}} - T_{\mathrm{w}}\right) \tag{S4}$$

where η can be 65 or 80, according to which metric we want to calculate. We use the same thresholds of T_w for them in this study.

The only metric derived from the physiology algorithm in this study is the Temperature Humidity Index for Physiology (THIP), which is calculated as:

$$\mathrm{THIP} = 0.63T_{\mathrm{w}} + 1.17T_{\mathrm{C}} + 32 \tag{S5}$$

THIP and THIC are both for livestock[28], and the equations we use in this study are specifically for pigs. For THIC and THIP, 75-78 means alert, 79-83 means dangerous, and 84+ means very dangerous.

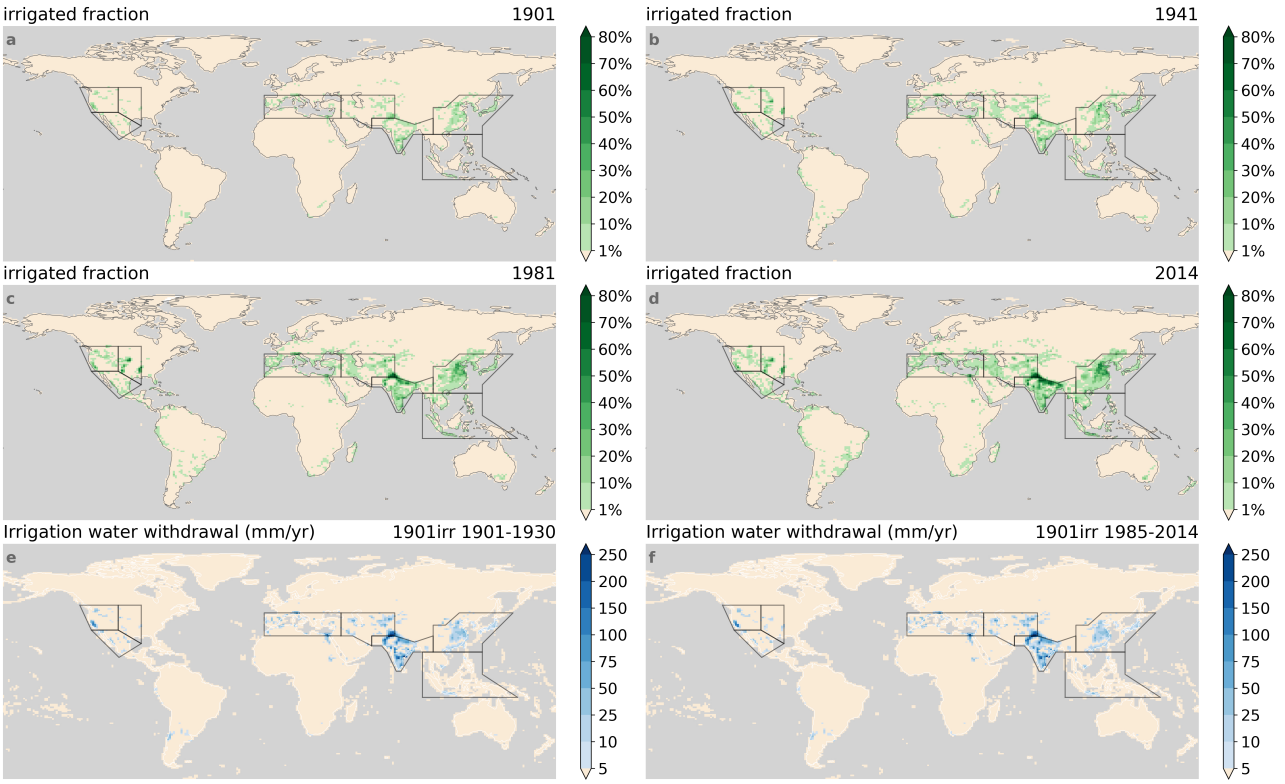
Discomfort Index (DI) was developed firstly as an air conditioner calibration[29], and the Israeli Defense Force used it to make decisions about heat stress[30]. It is calculated as the average value of T_w and T_C:

$$\mathrm{DI} = 0.5T_{\mathrm{w}} + 0.5T_{\mathrm{C}} \tag{S6}$$

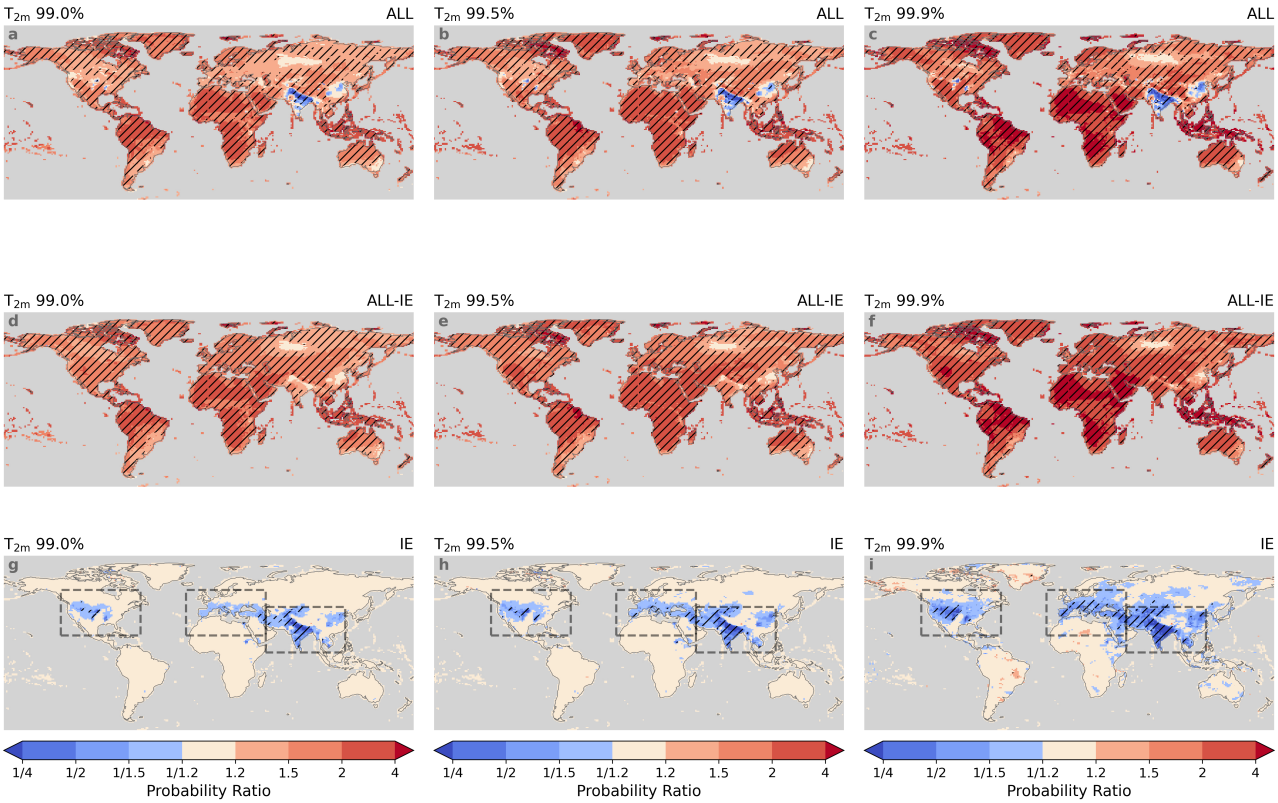
For DI, we use a series of thresholds: 21-24 means <50 % of people feel discomfort, 24-27 means >50 % of people feel comfort, 27 - 29 means most of the people feel discomfort, and 29-32 and >32 mean severe stress and emergency, respectively[31].

2 Supplementary Figures

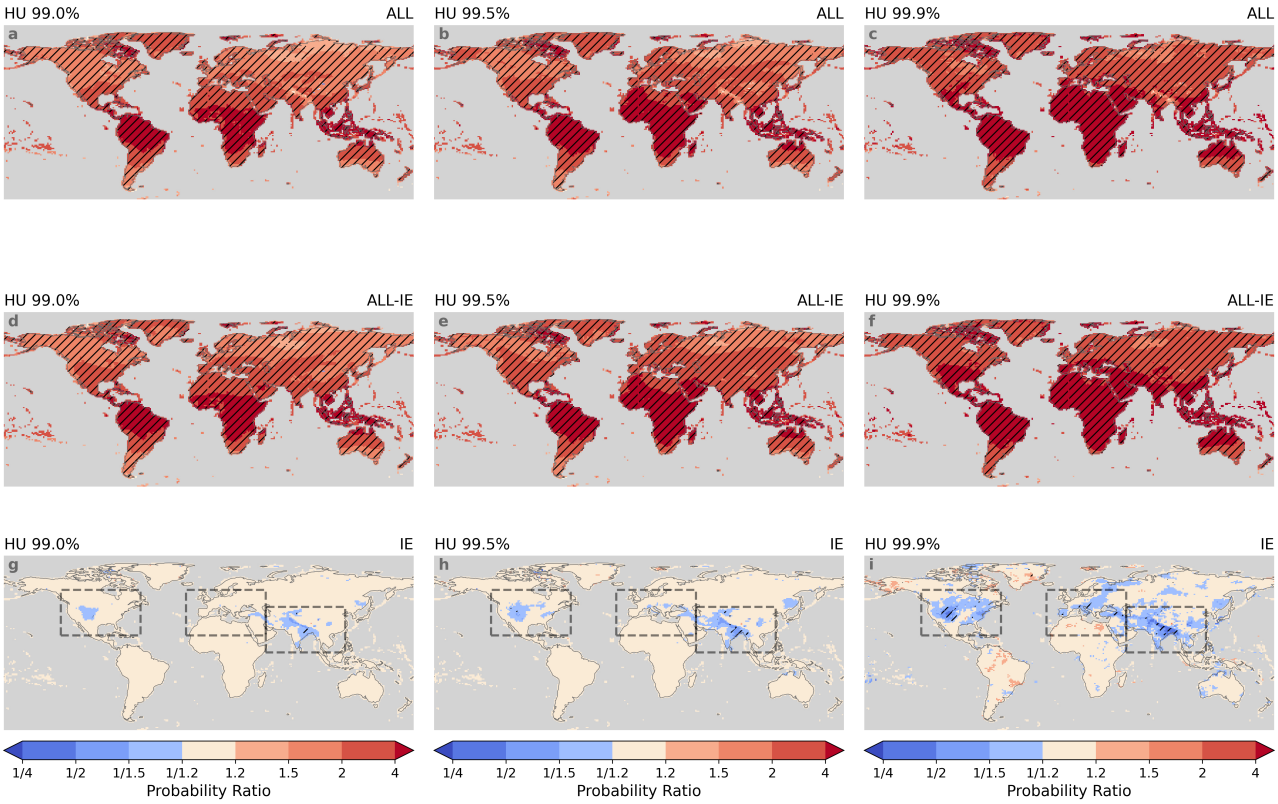
2.1 Supplementary Figures 1: Appendix Figures



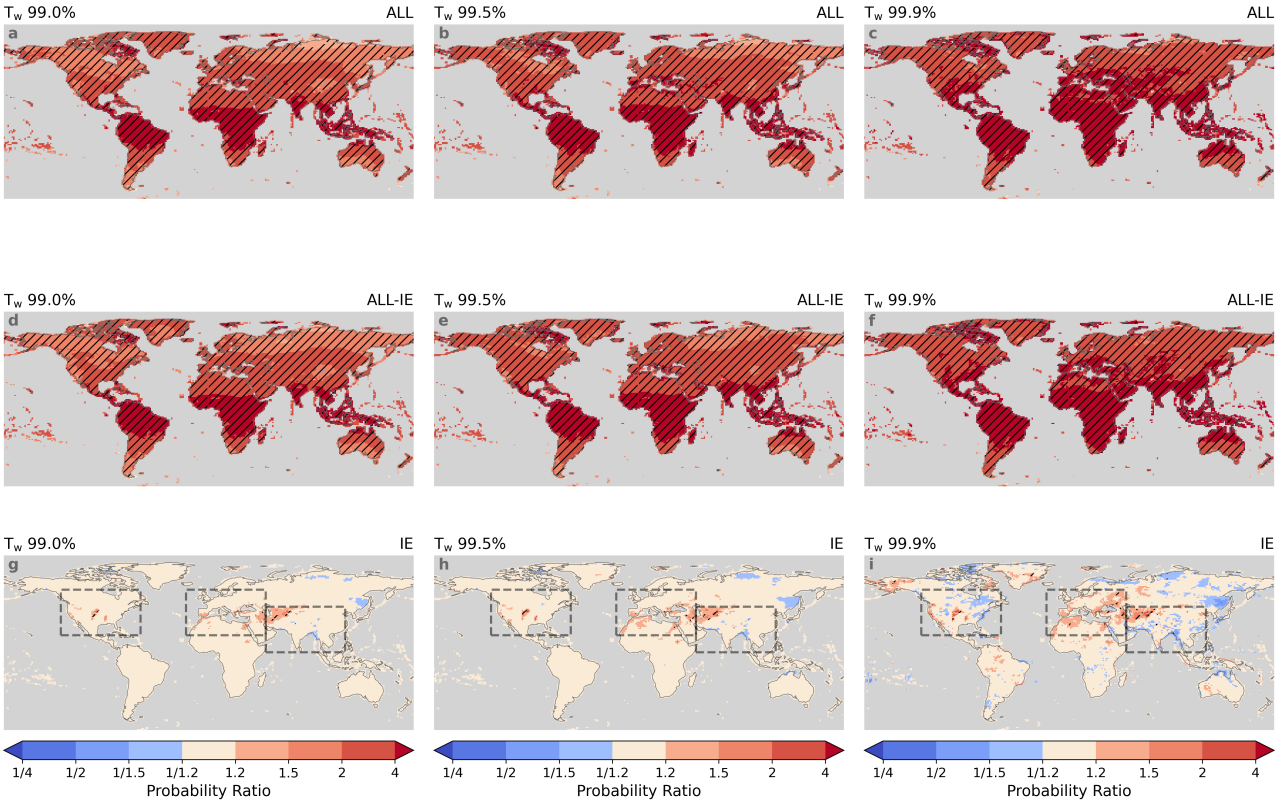
Supplementary Figure S3 | **a-d** Irrigated fraction in the year 1901 (**a**), 1941 (**b**), 1981 (**c**), and 2014 (**d**). **e-f** Multi-model mean simulated annual irrigation water withdrawal without transient irrigation (*1901irr*) extent during the first 30 years (1901-1930: **c**) and the last 30 years (1985-2014: **d**). IPSL-CM6 does not run the 1901irr experiment with fixed irrigation extent (see Method), so the values shown here are the average value of other five models (CESM2, CESM2_gw, NorESM2, E3SMv2, and CNRM-CM6-1.



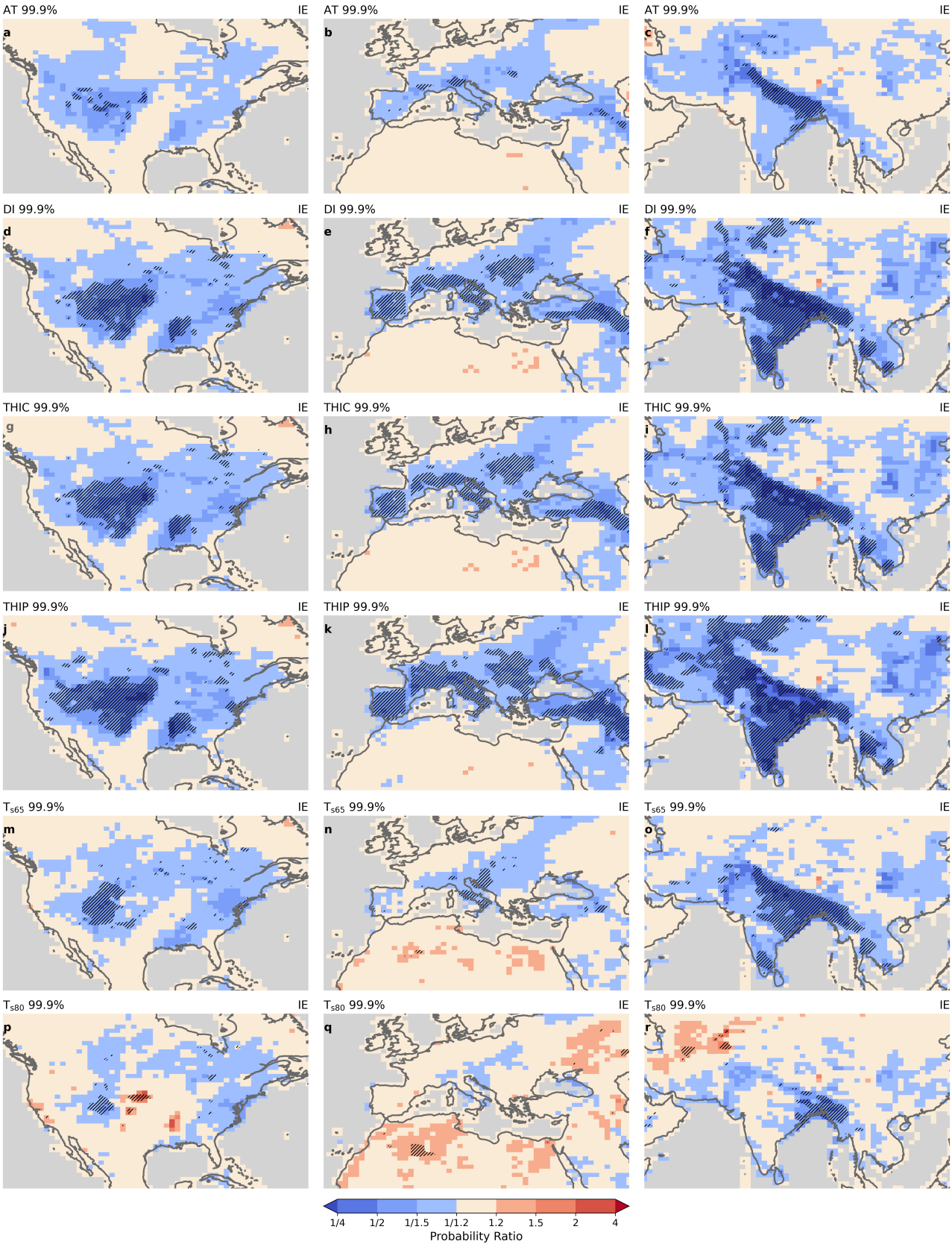
Supplementary Figure S4 | **a-c** Multi-model mean absolute values of the 99th (**a**), 99.5th (**b**), and 99.9th (**c**) percentile values of 2-meter air temperature of the first 30 years (1901-1930) in the simulations without irrigation expansion (*1901irr*). **d-l** Multi-model mean impacts of all forcings (ALL: greenhouse gas emissions, land use and land management change, irrigation expansion, etc.) (**d,e,f**), all forcings except irrigation expansion (ALL-IE: **g,h,i**), and irrigation expansion (IE: **j,k,l**) on the 99th (**d, g, j**), 99.5th (**e, h, k**), and 99.9th (**f,i,l**) percentile values of T_{2m}. Impacts are calculated by subtracting the values in the new exp_period by those in the reference exp_period (see Table 1 in main text). Hatches indicate that signals (>0.1 or <-0.1) are agreed by $\geq$ 5 of 6 models (results of individual models can be found in Supplementary Figures 1).



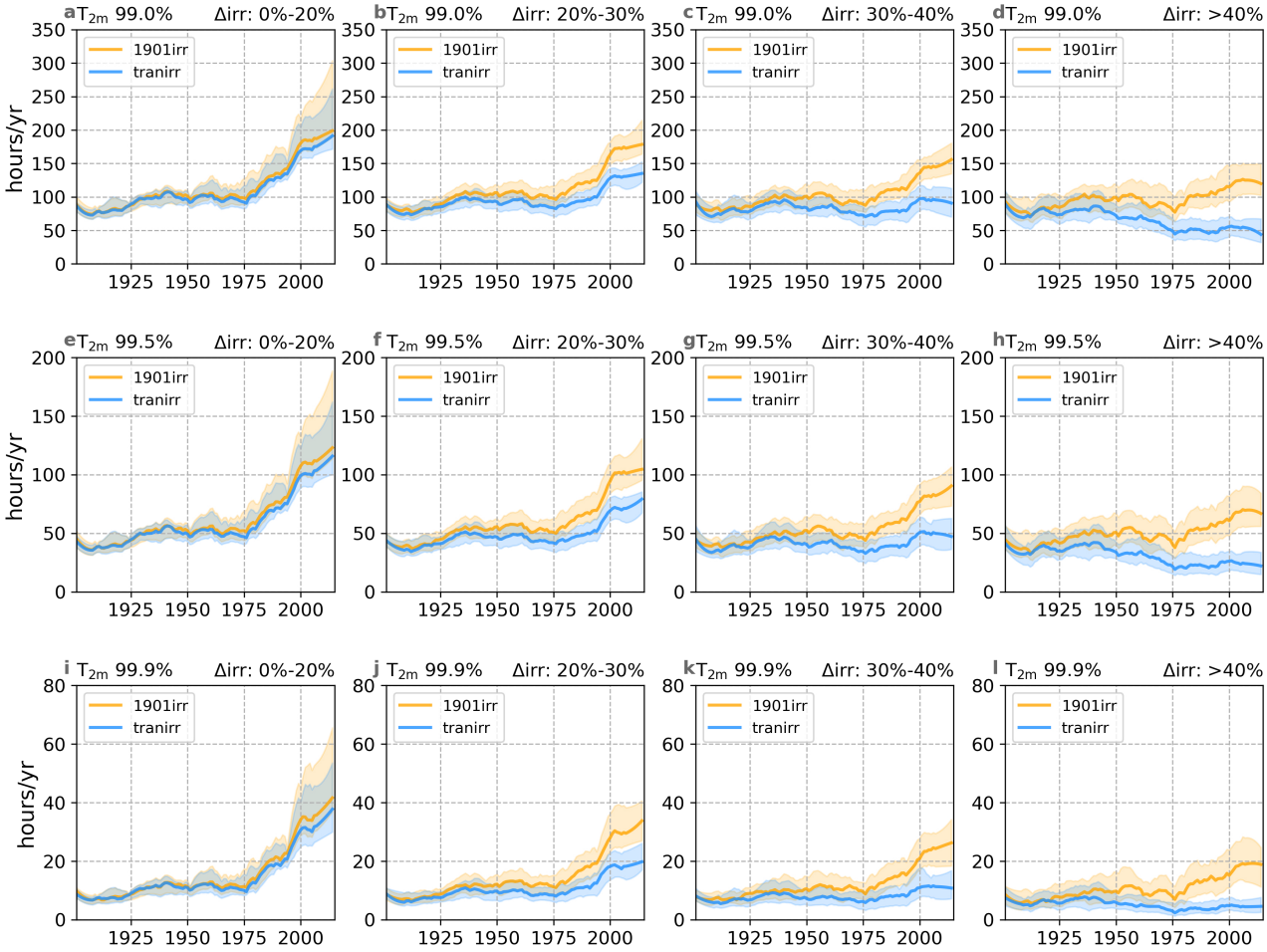
Supplementary Figure S5 | Same as Figure S4 but for HUMIDEX (HU).



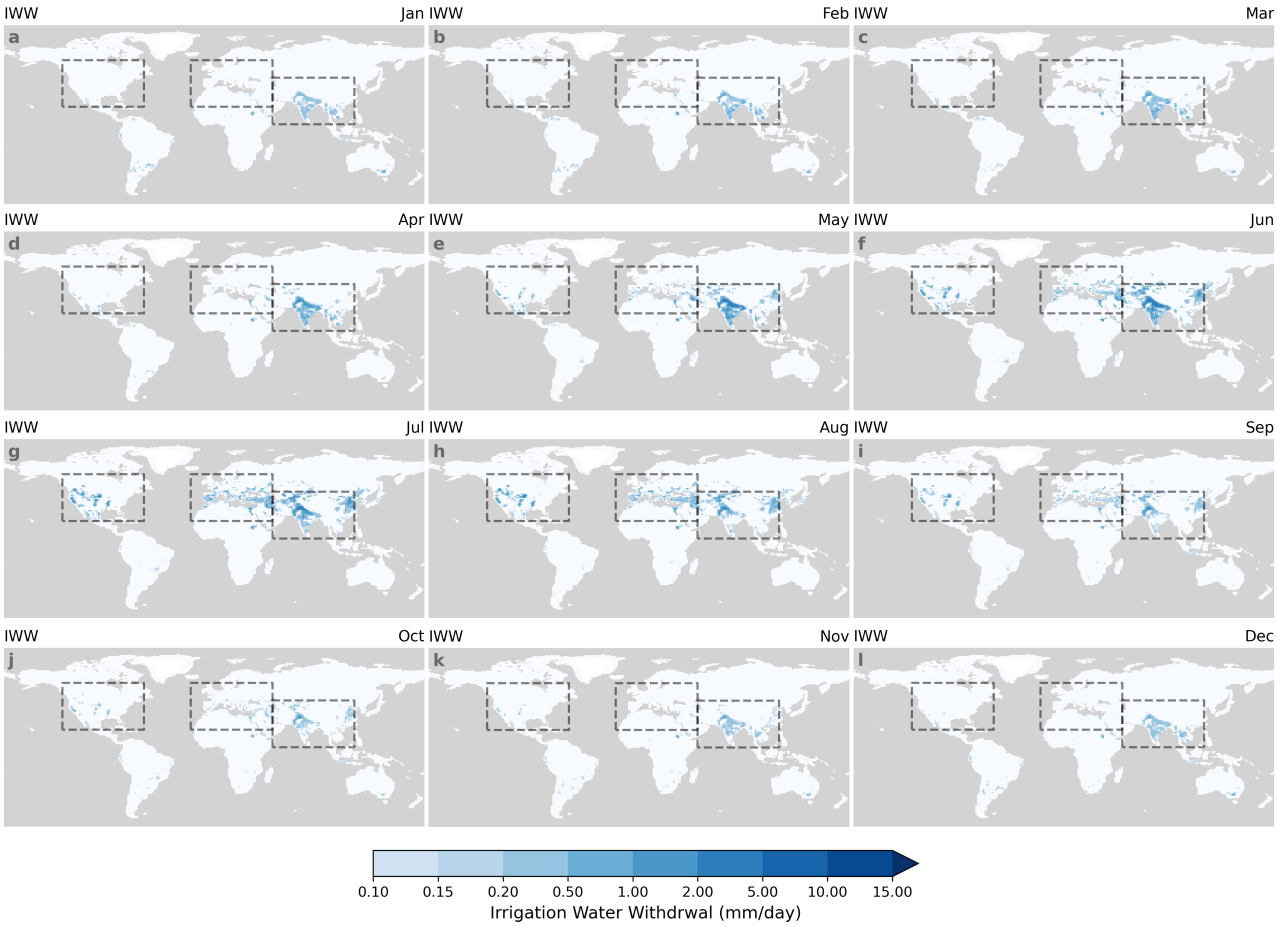
Supplementary Figure S6 | Same as Figure S4 but for wet-bulb temperature (T_w).



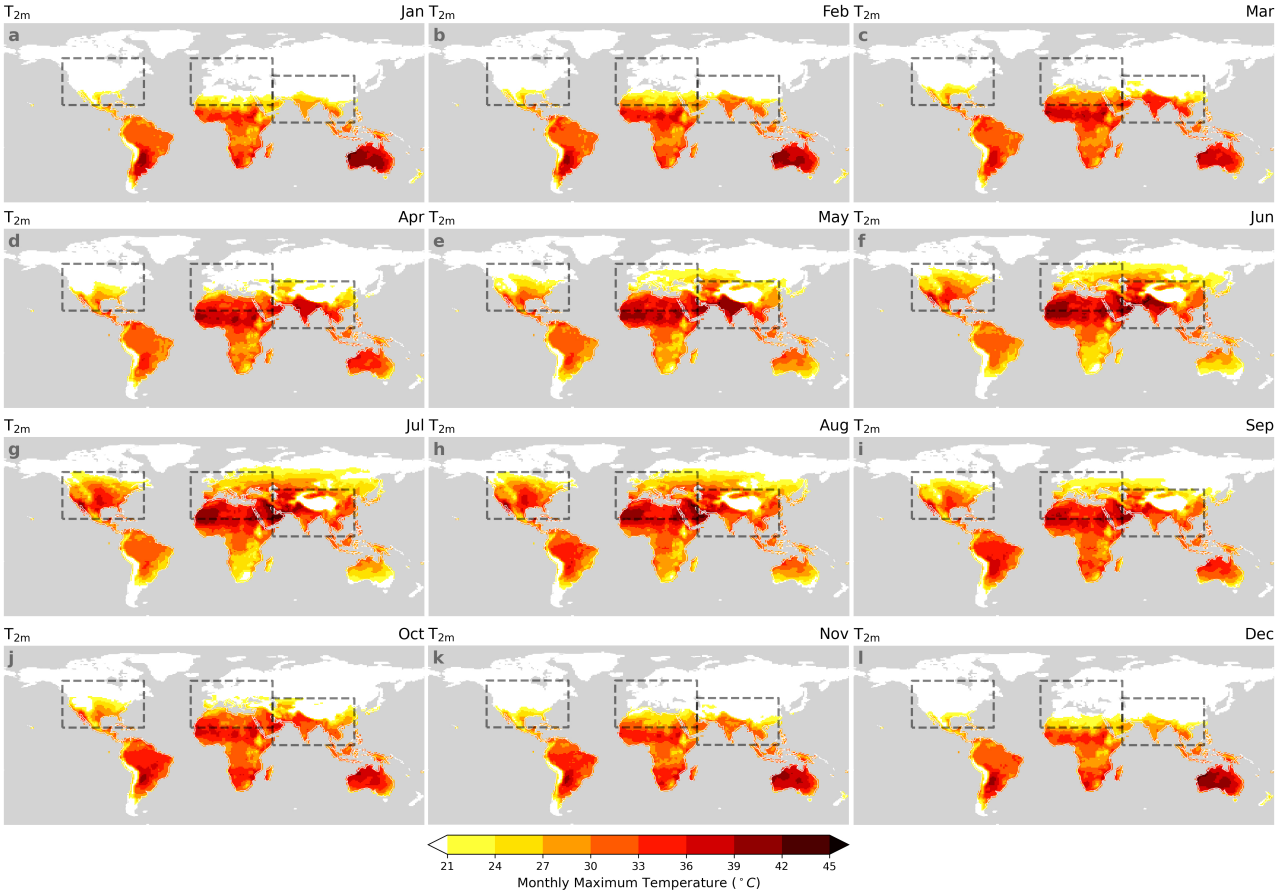
Supplementary Figure S7 | Impacts of irrigation expansion (IE) on the frequency of the events in which Apparent Temperature (AT: **a-c**), Discomfort Index (DI: **d-f**), Temperature Humidity Index for Comfort (THIC: **g-i**), Temperature Humidity Index for Physiology (THIP: **j-l**), temperature when 65 % (T_{s65}: **m-o**) and 80 % (T_{s80}: **p-r**) of the swamp coolers are approached exceed their 99.9th percentile values of the first 30 years (1901-1930) in the simulations without irrigation expansion (*1901irr*). Hatches indicate that signals (>1.2 or <1/1.2) are agreed by $\geq$ 5 of 6 models, except for AT, for which hatches mean that signals are agreed by $\geq$ 4 of 5 models (except CNRM-CM6-1).



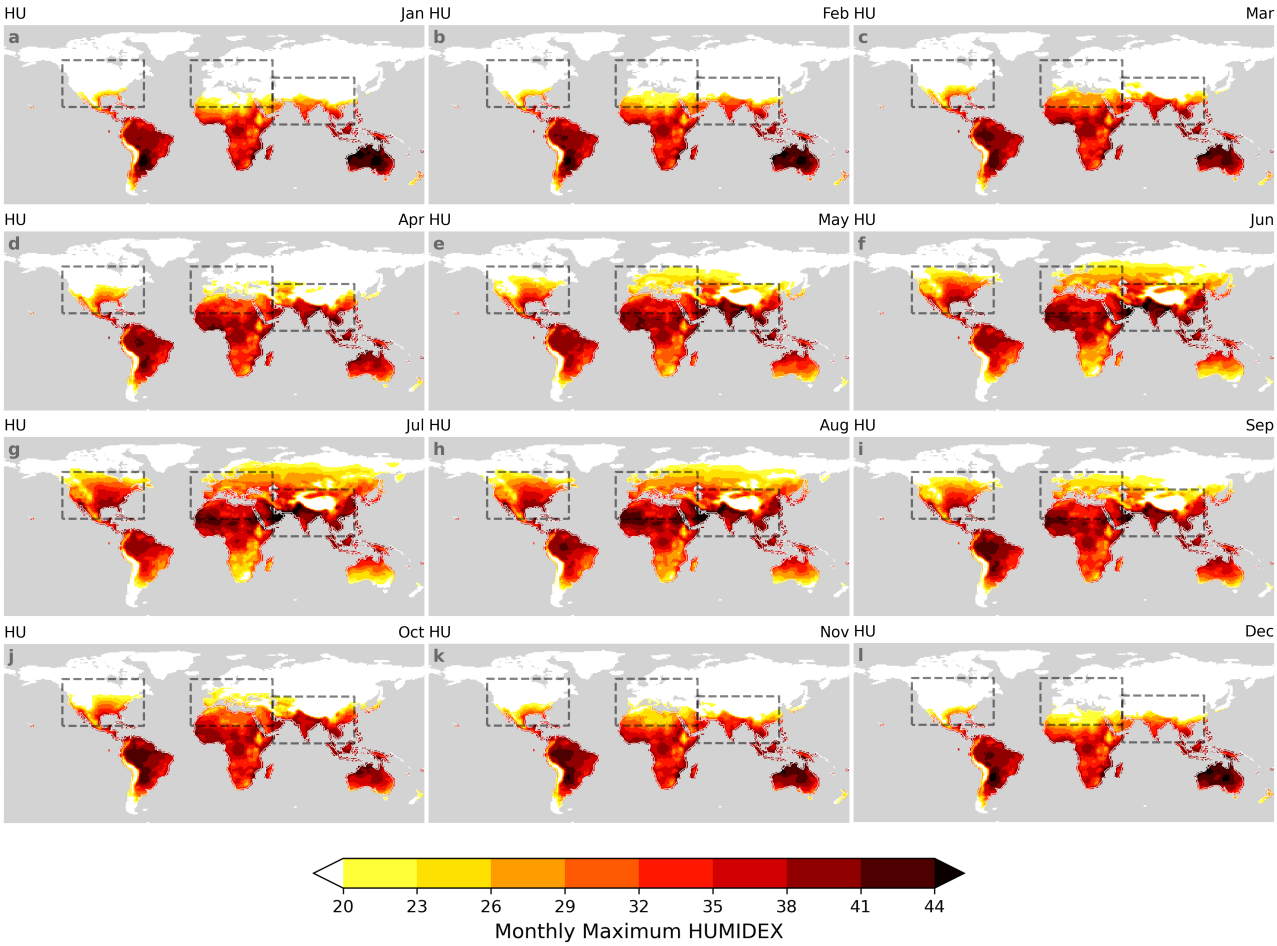
Supplementary Figure S8 | Time series of the annual hours exposed to 99^{th} (**a-d**), 99.5^{th} (**e-h**), and 99.9^{th} (**i-l**) percentile extremes of 2-meter air temperature (T_{2m}) over grid cells with irrigation expansion of 0-20% (**a, e, i**), 20%-30% (**b, f, j**), 30%-40% (**c, g, k**) and >40% (**d, h, i**). Curves were smoothed using Savitzky-Golay filtering (order = 2, window = 15)[1]. Results of HUMIDEX and wet-bulb temperature can be found in Supplementary Figures 2.



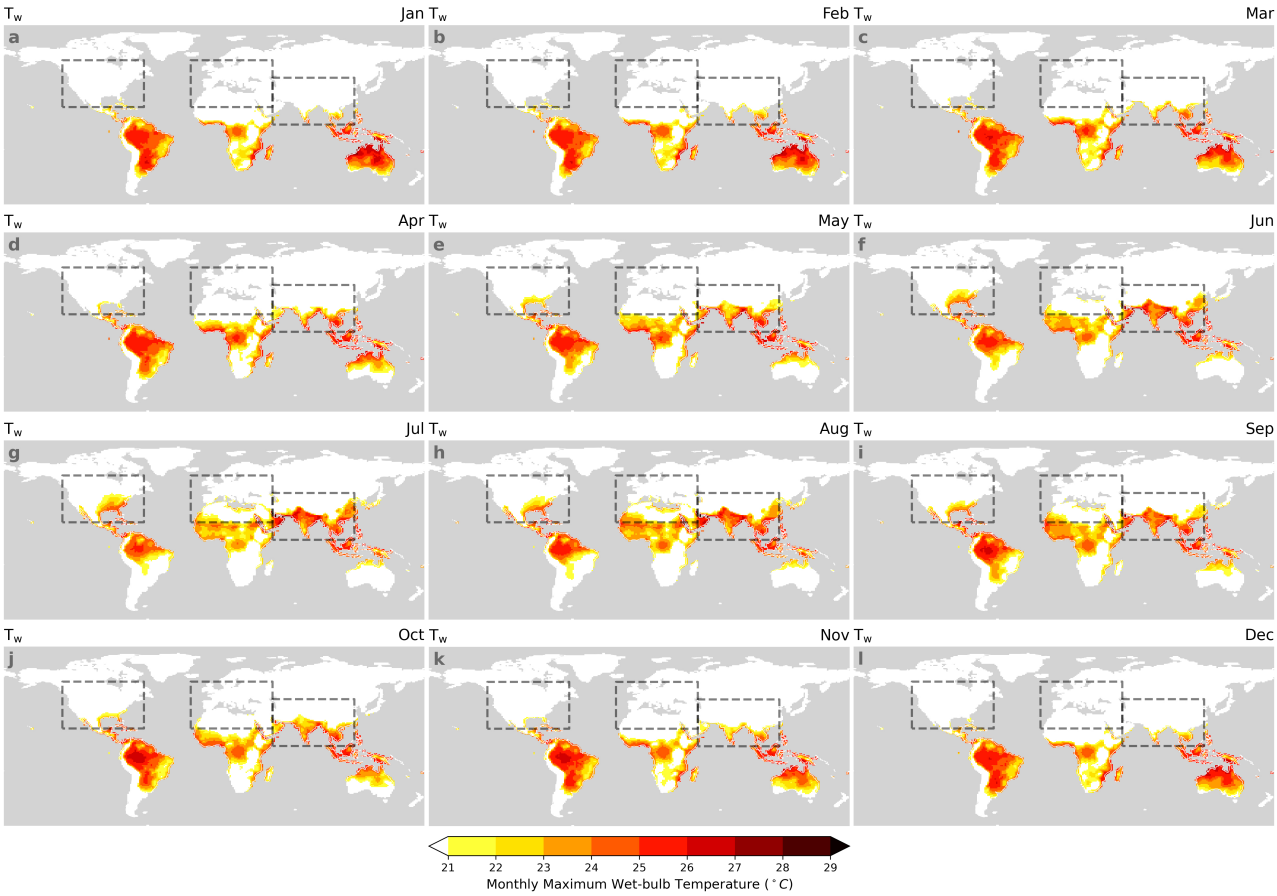
Supplementary Figure S9 | Multi-year mean monthly irrigation water withdrawal (IWW) during the period 1985-2014 of the experiment with irrigation expansion (*tranirr*). Results shown are average values of all six models.



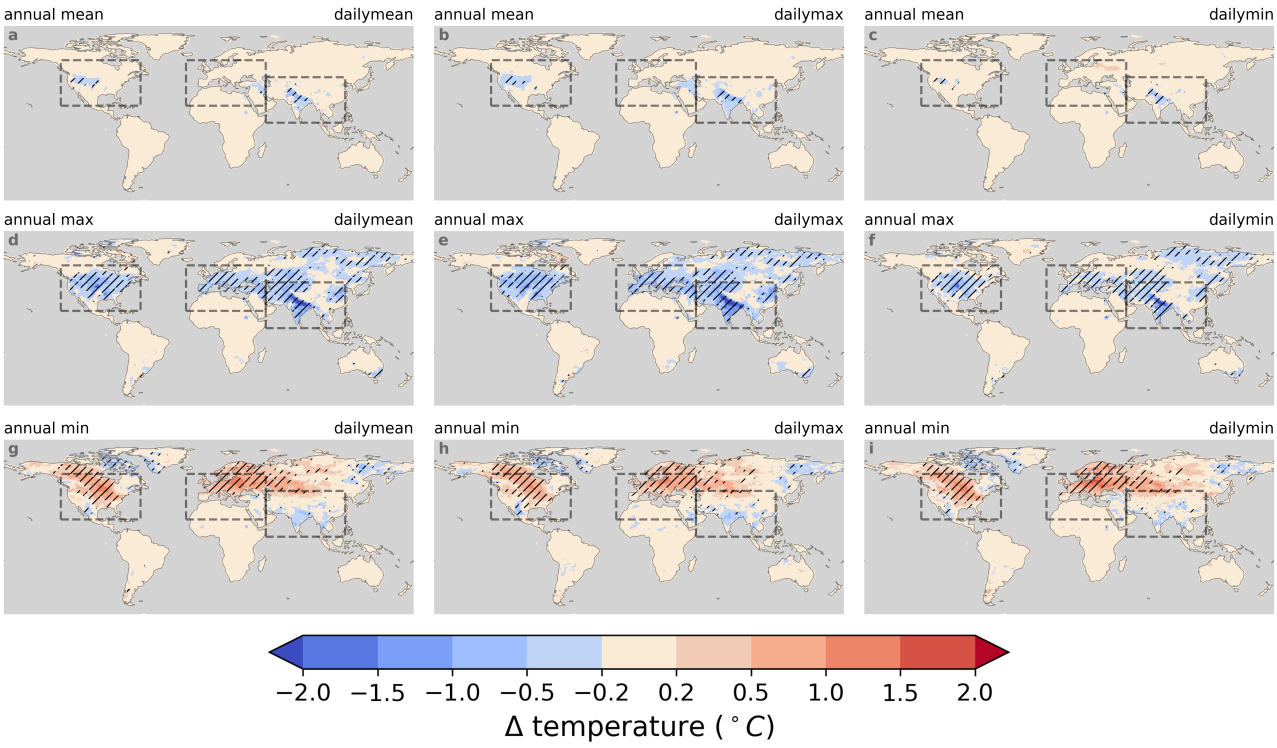
Supplementary Figure S10 | Multi-year mean monthly maximum 2-meter air temperature (T_{2m}) during the period 1985-2014 of the experiment without irrigation expansion (*1901irr*). Results shown are average values of all six models.



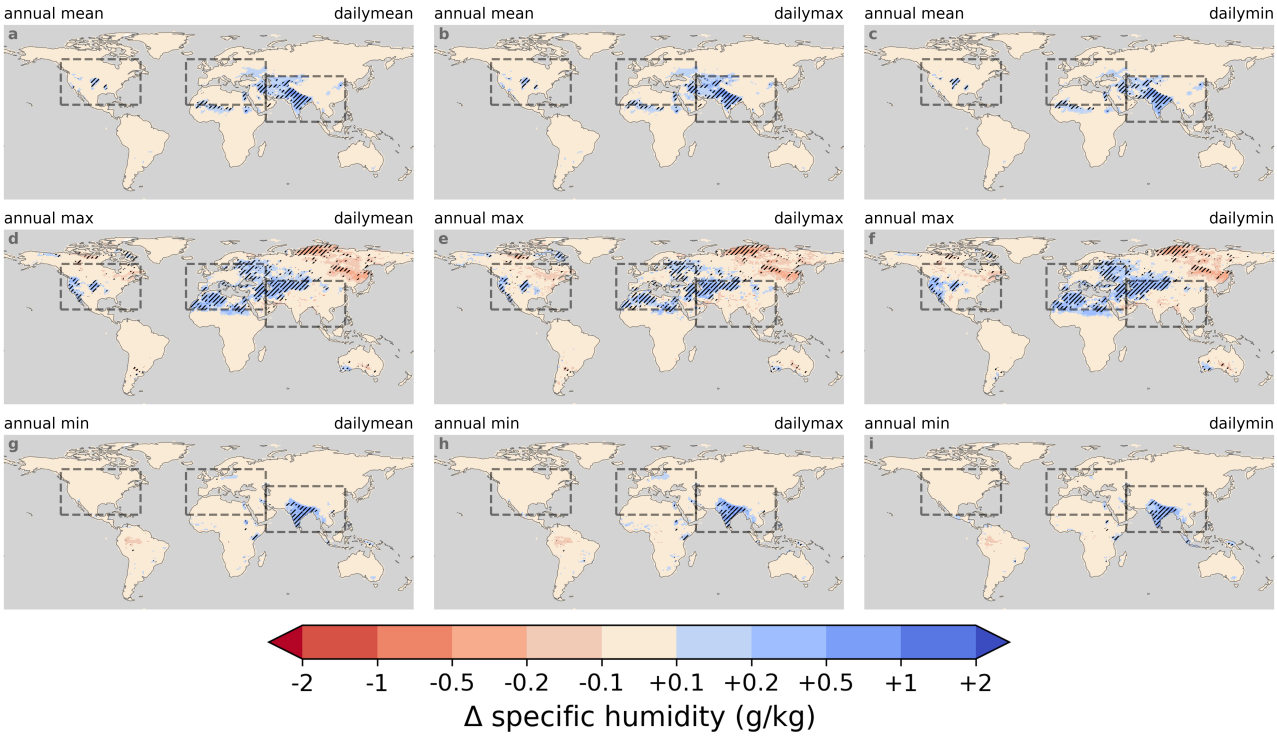
Supplementary Figure S11 | Similar to Figure S10 but for HUMIDEX (HU).



Supplementary Figure S12 | Similar to Figure S10 but for wet-bulb temperature (T_w).

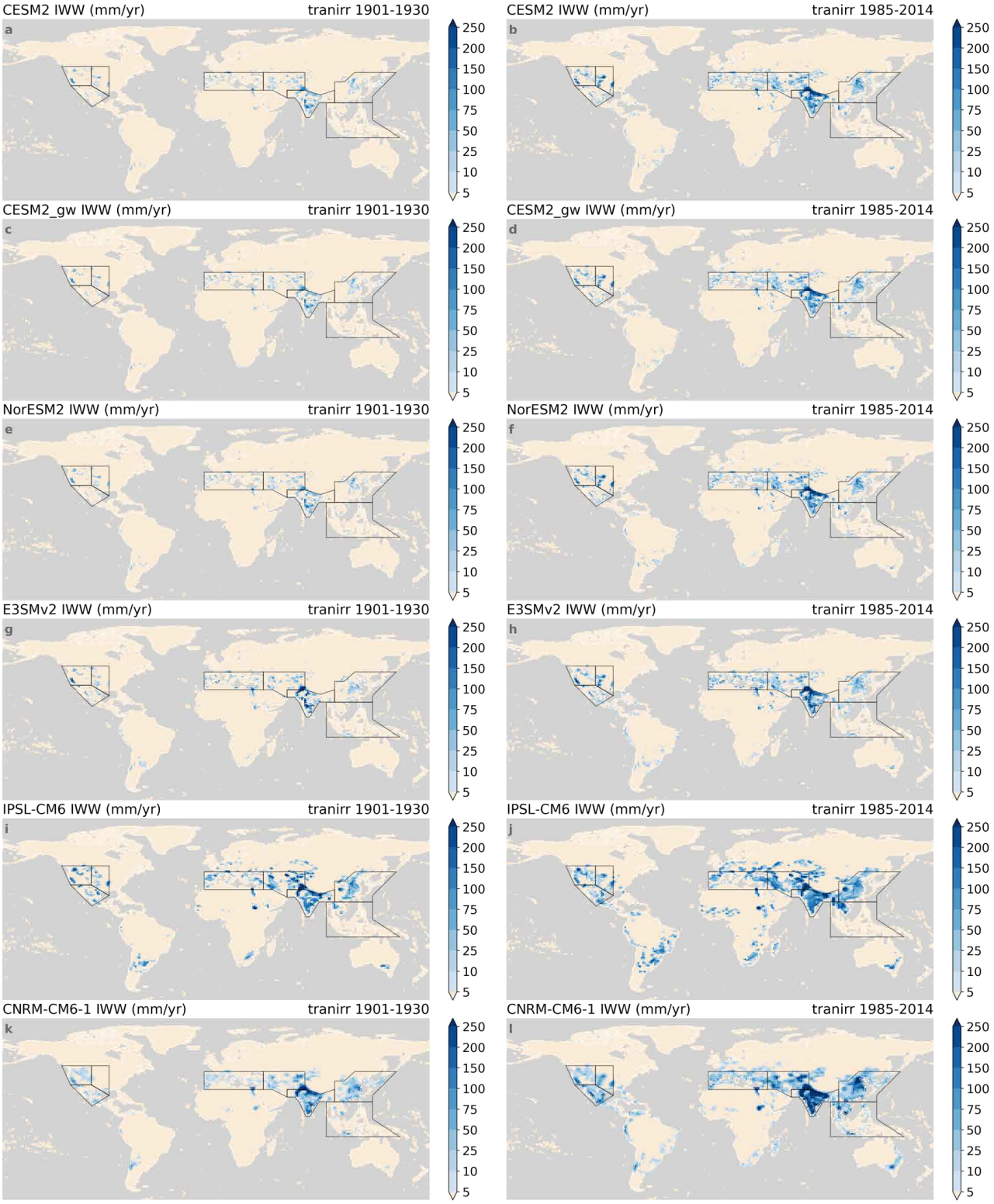


Supplementary Figure S13 | Impacts of irrigation expansion (IE) on the annual mean (**a, b, c**), annual maximum (**d, e, f**) and annual minimum (**a, d, g**) values of the daily mean (**a, d, g**), daily maximum (**b, e, h**), and daily minimum (**b, e, h**) 2-meter air temperature (T_{2m}).

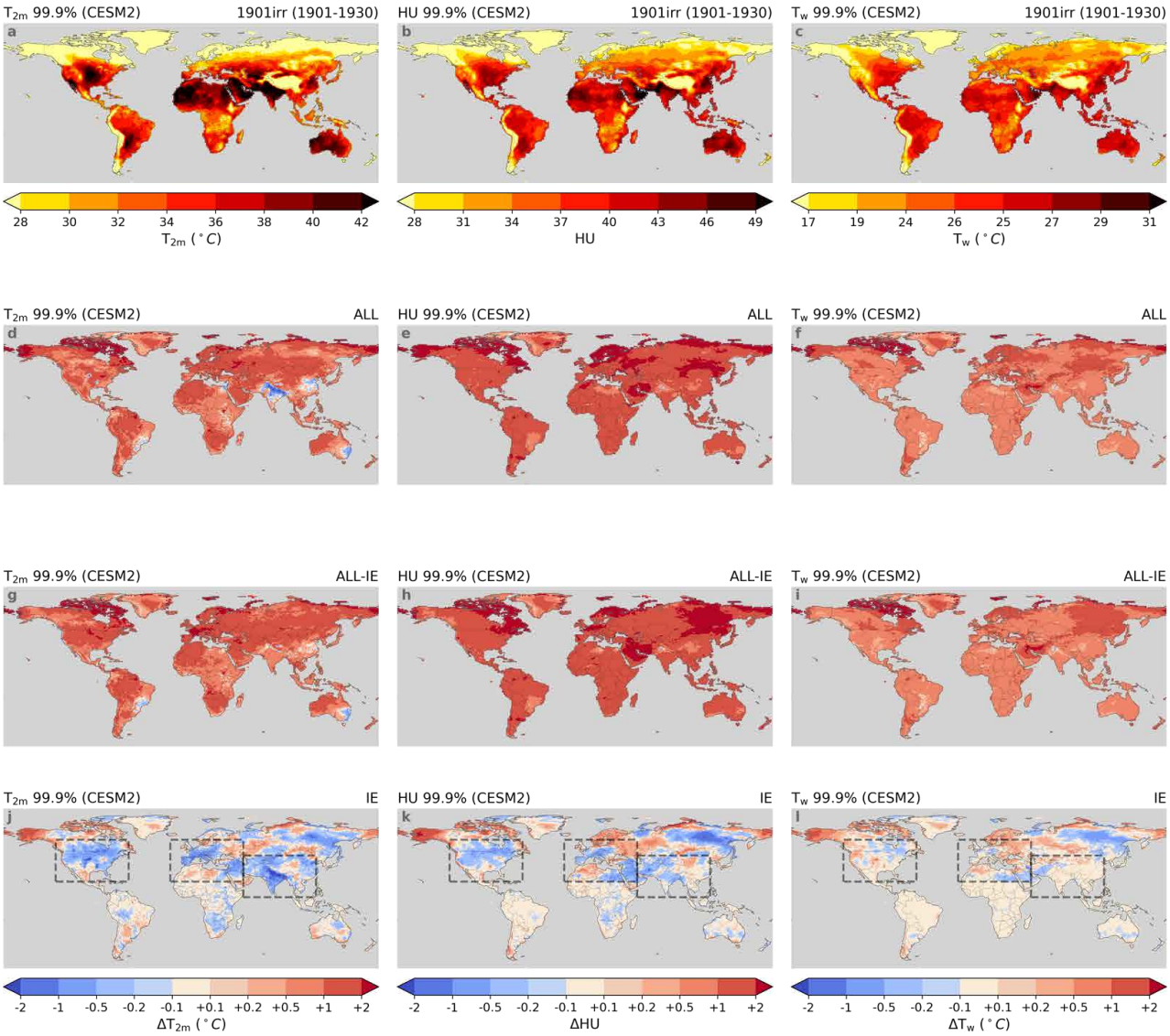


Supplementary Figure S14 | Same as Figure S13 but for specific humidity.

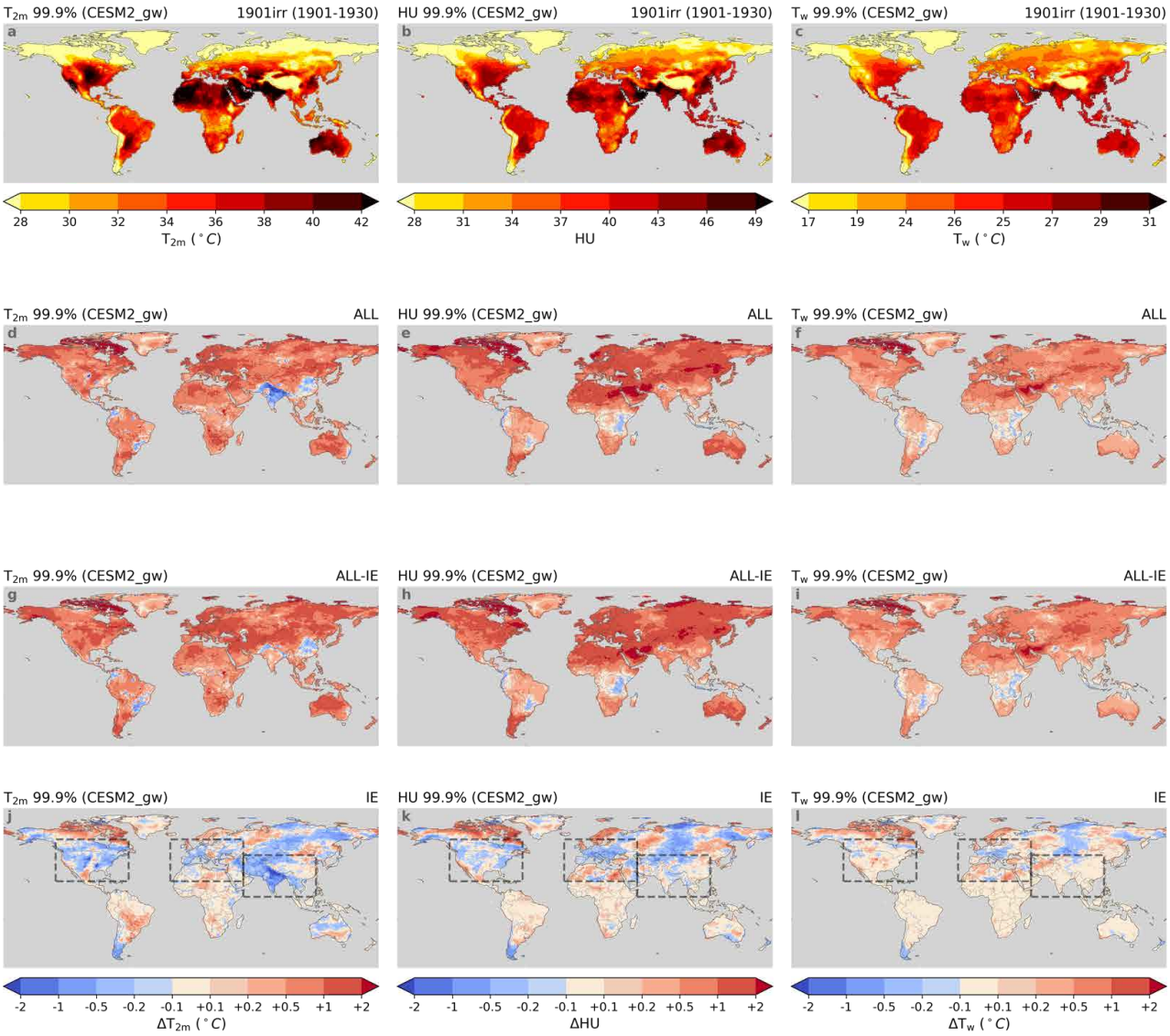
2.2 Supplementary Figures 2: Results of individual ESMs



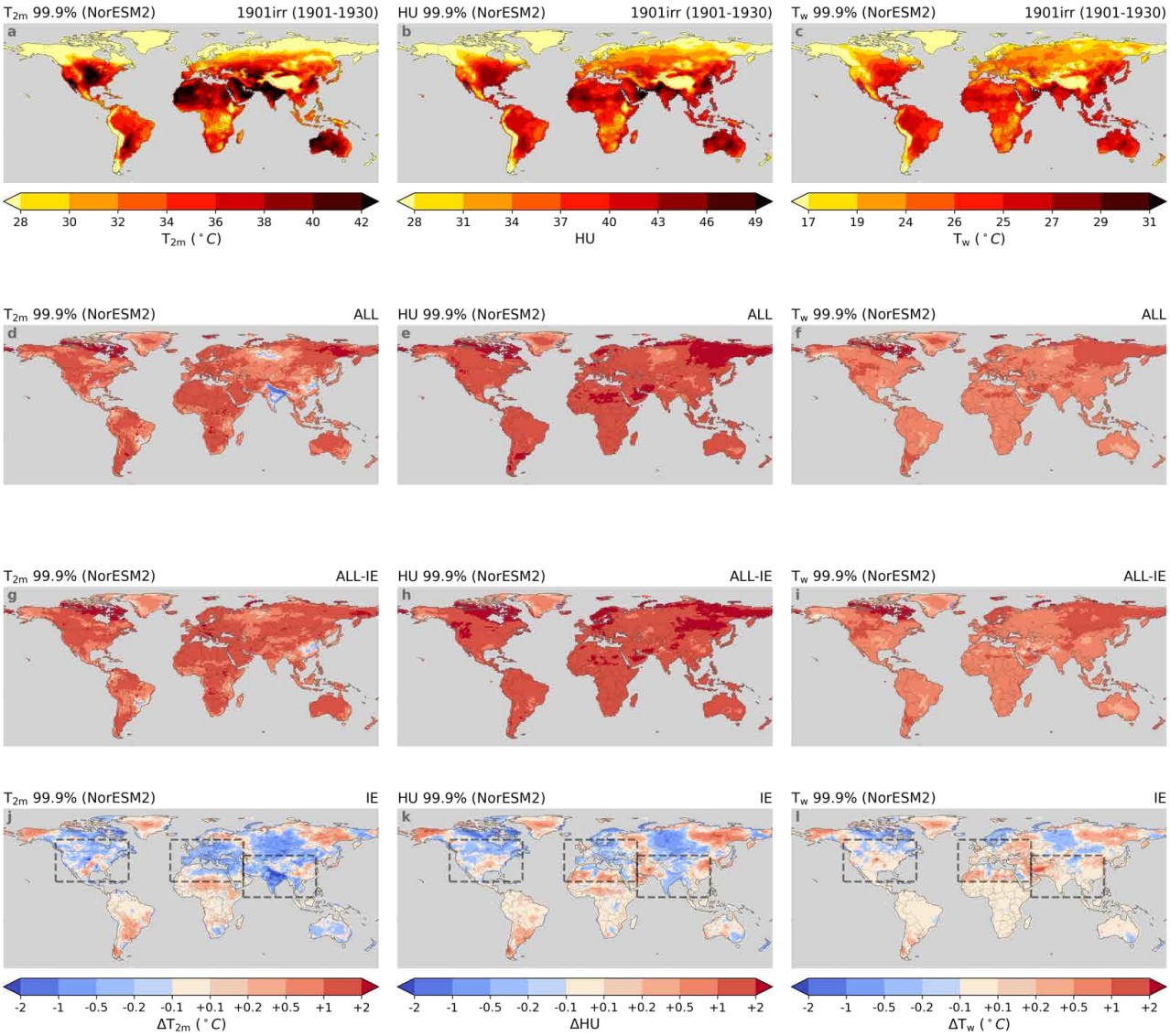
Supplementary Figure S15 | Simulated annual irrigation water withdrawal (IWW) with transient irrigation (tranirr) extent during the first 30 years (1901-1930: **left**) and the last 30 years (1985-2014: **right**).



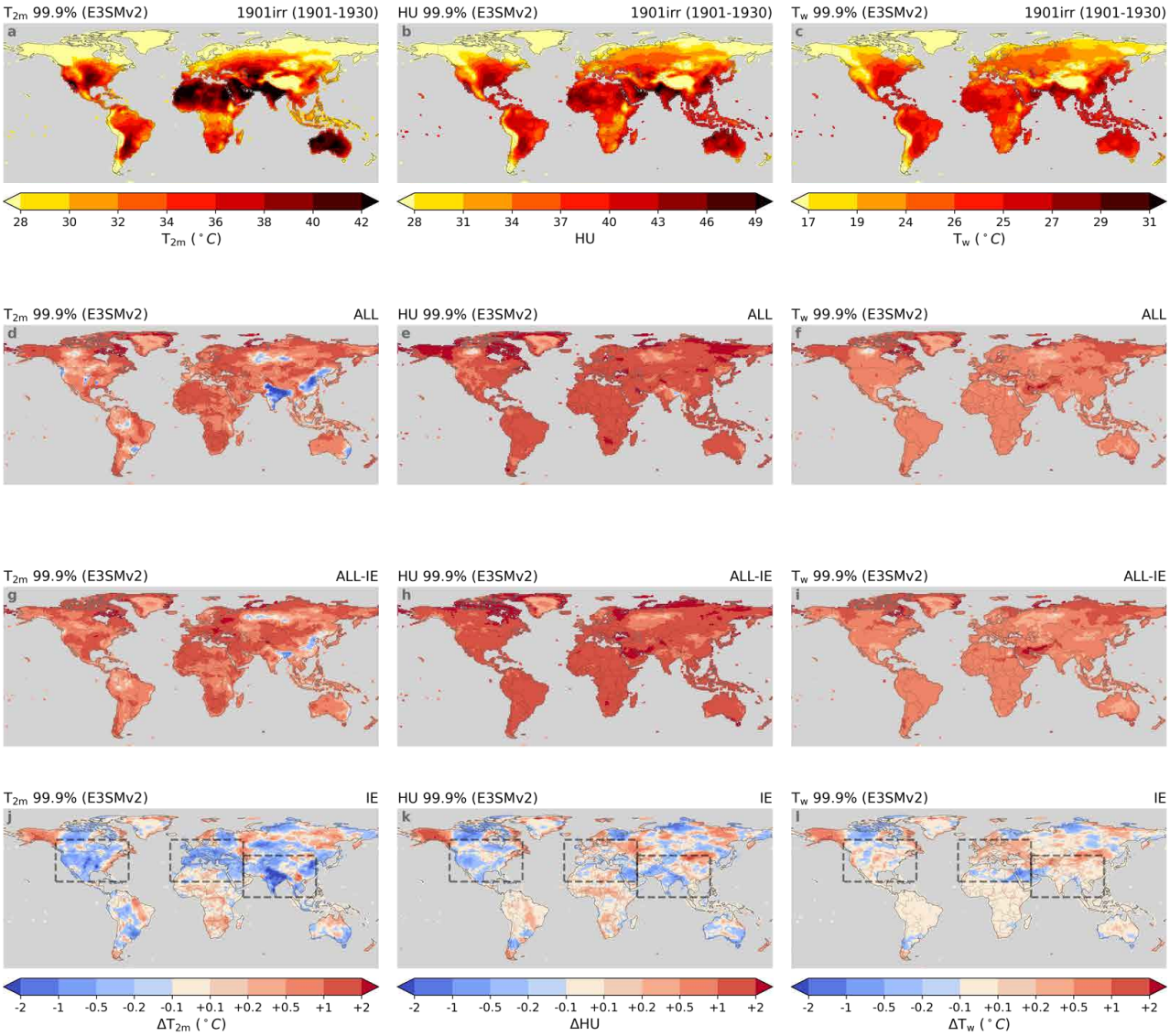
Supplementary Figure S16 | **a-c** Multi-ensemble member mean absolute values of the 99.9th percentile values of 2-meter air temperature (T_{2m}: **a**), HUMIDEX (HU: **b**), and wet-bulb temperature (T_w: **c**) of the first 30 years (1901-1930) in the simulations without irrigation expansion (*1901irr*) calculated based on CESM2 outputs. **d-l** Multi-ensemble member mean impacts of all forcings (ALL: greenhouse gas emissions, land use and land management change, irrigation expansion, etc.) (**d, e, f**), all forcings except irrigation expansion (ALL-IE: **g, h, i**), and irrigation expansion (IE: **j, k, l**) on the 99.9th percentile values of T_{2m} (**d, g, j**), HU (**e, h, k**), and T_w (**f, i, l**) calculated based on CESM2 outputs. Impacts are calculated by subtracting the values in the new exp_period by those in the reference exp_period (see Table 1 in main text).



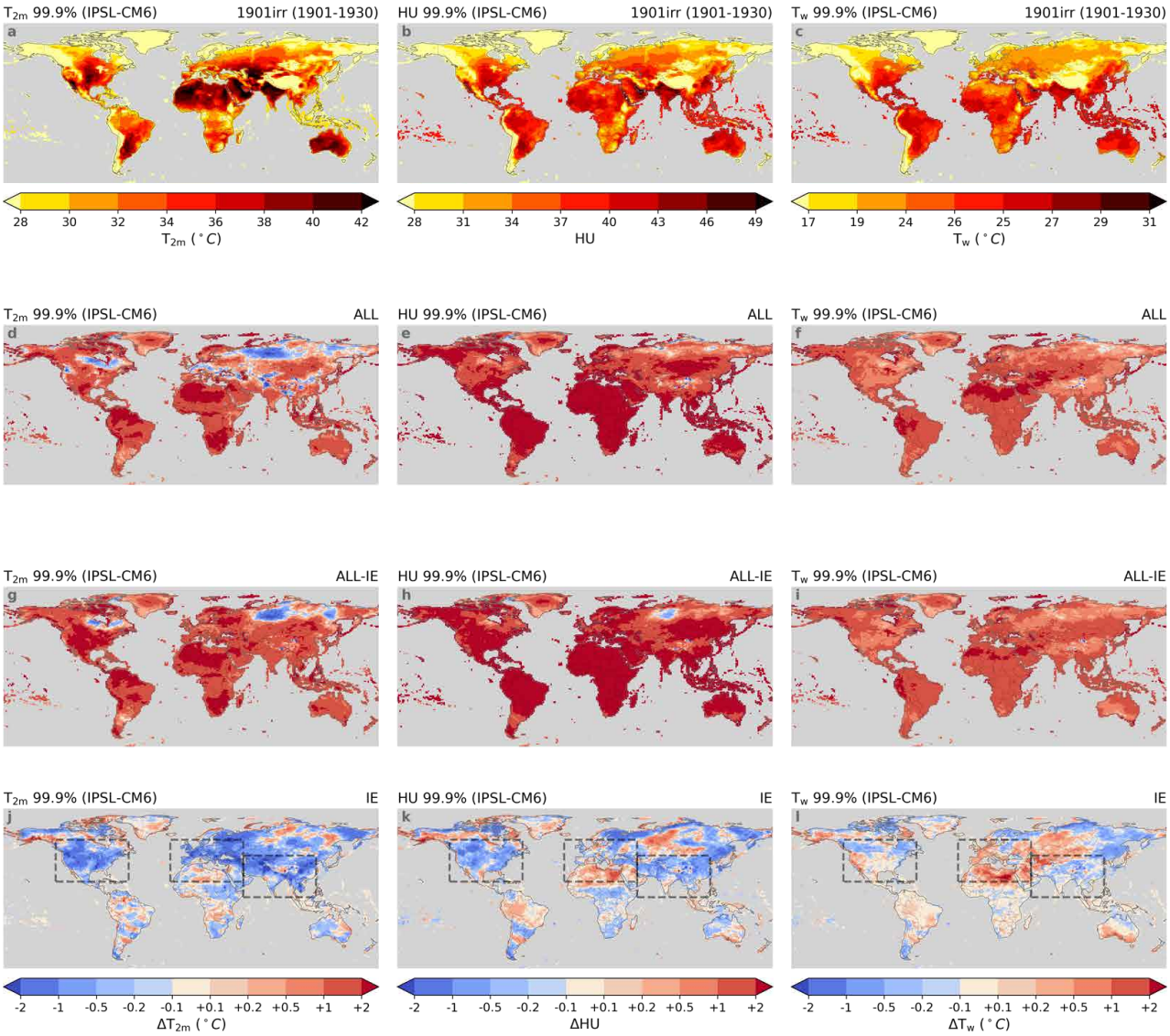
Supplementary Figure S17 | Same as Figure S16 but calculated based on CESM2_gw outputs.



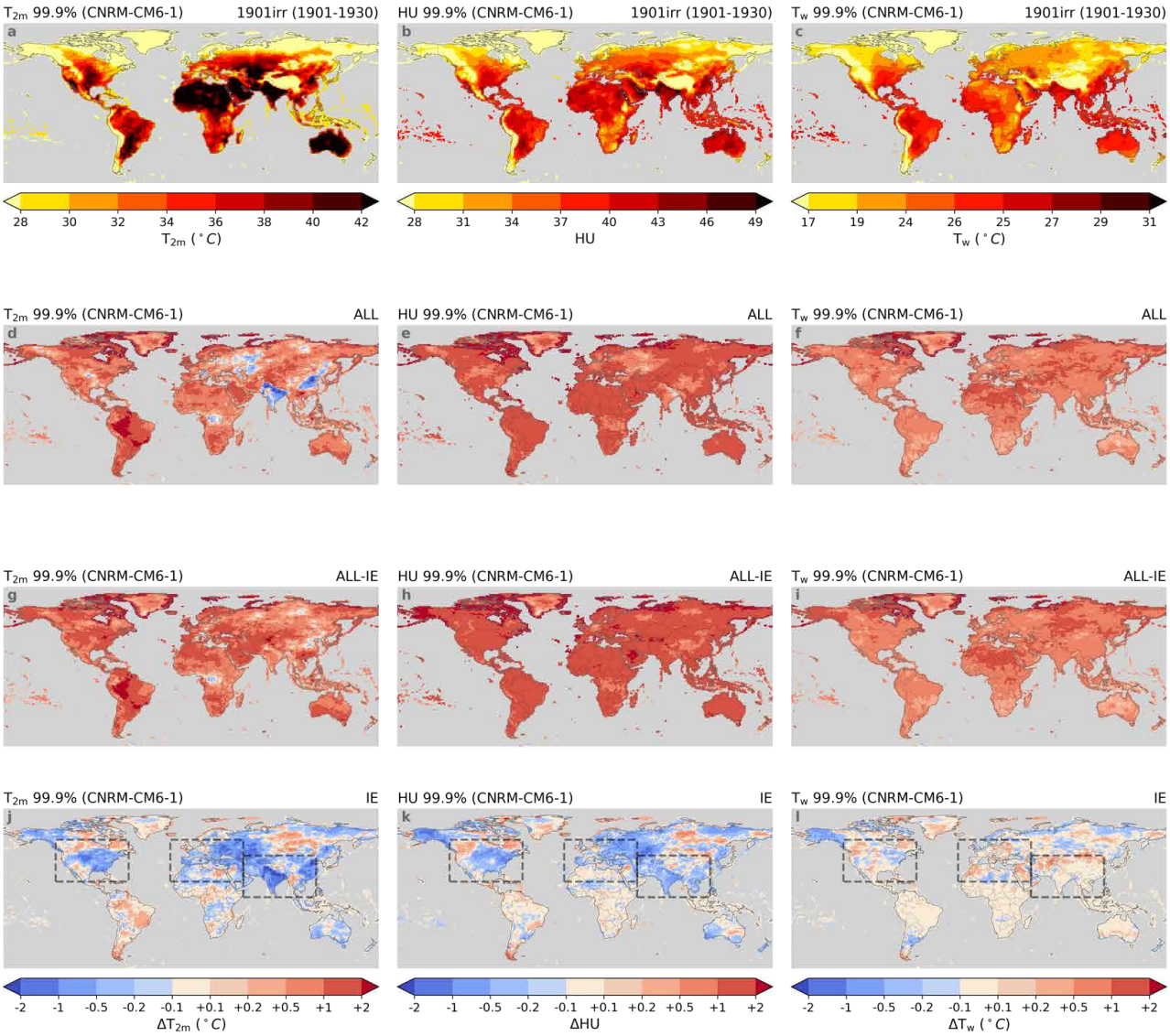
Supplementary Figure S18 | Same as Figure S16 but calculated based on NorESM2 outputs.



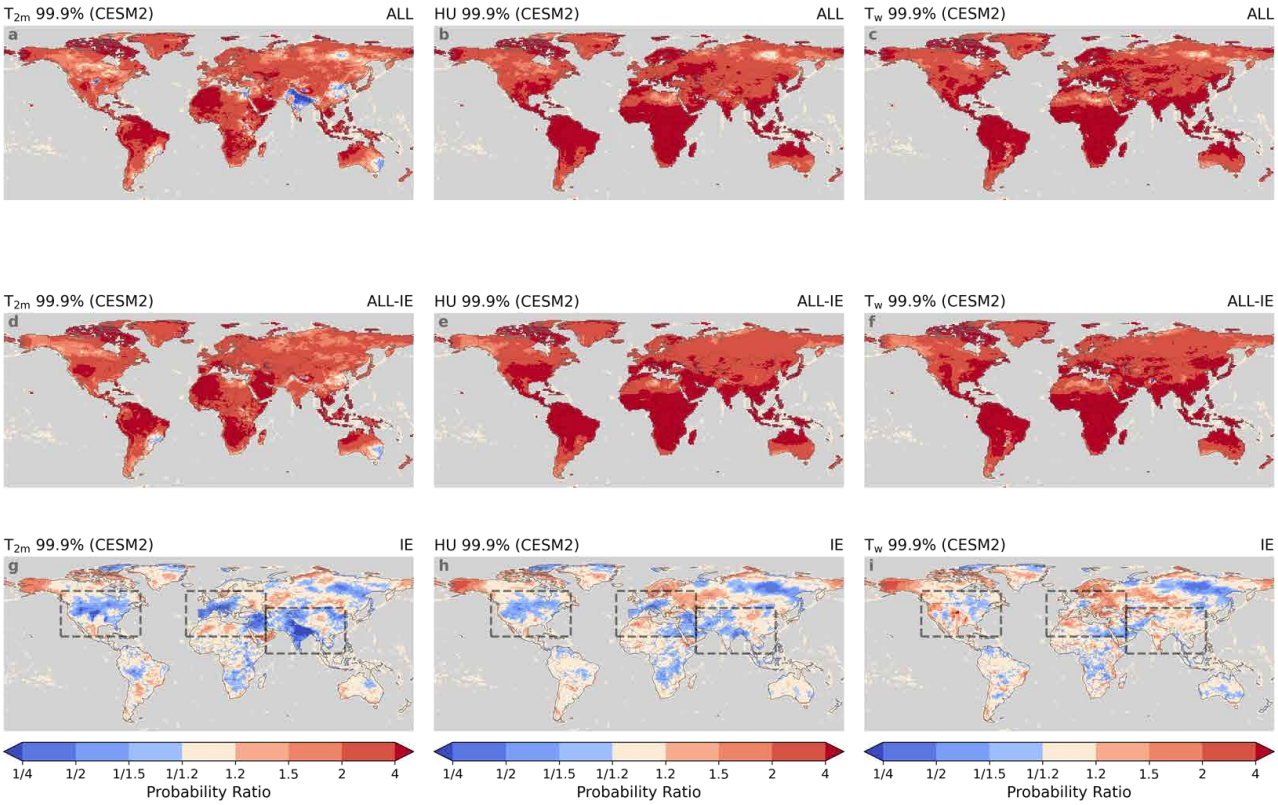
Supplementary Figure S19 | Same as Figure S16 but calculated based on E3SMv2 outputs.



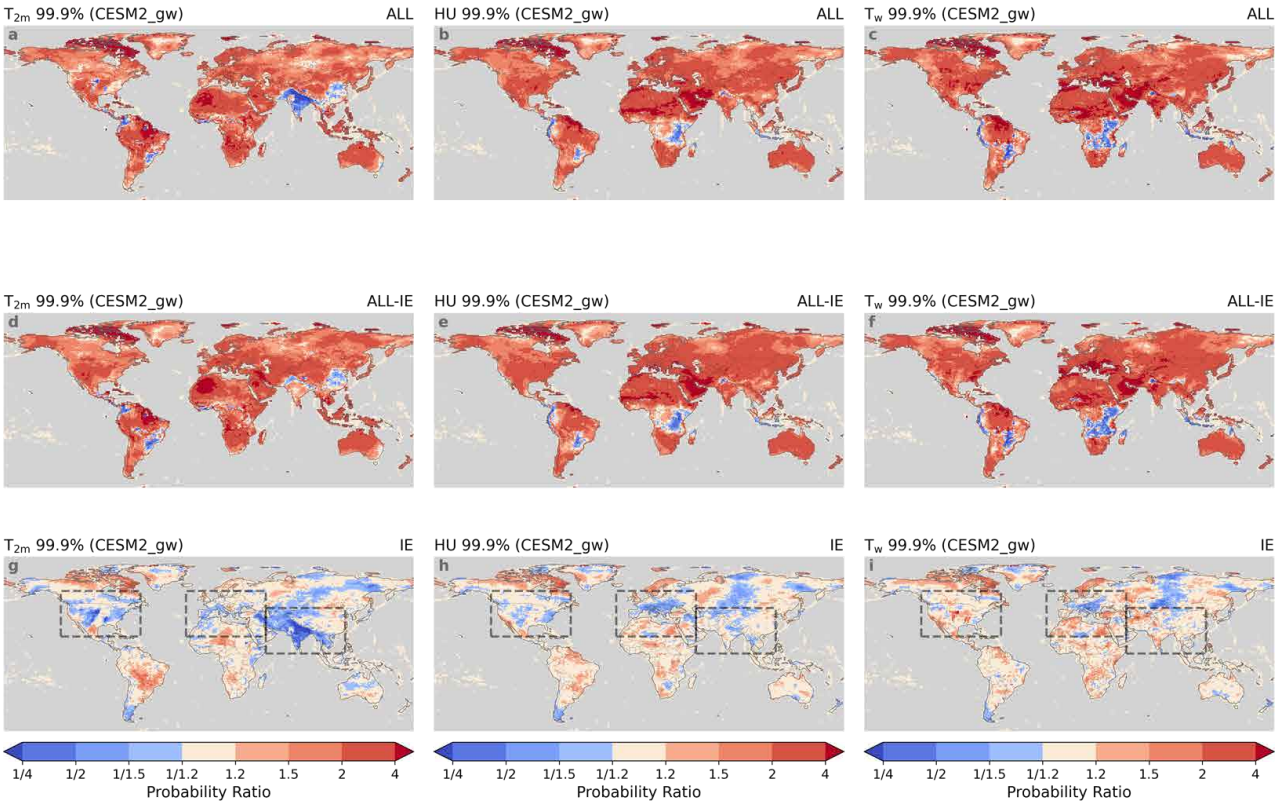
Supplementary Figure S20 | Same as Figure S16 but calculated based on IPSL-CM6 outputs.



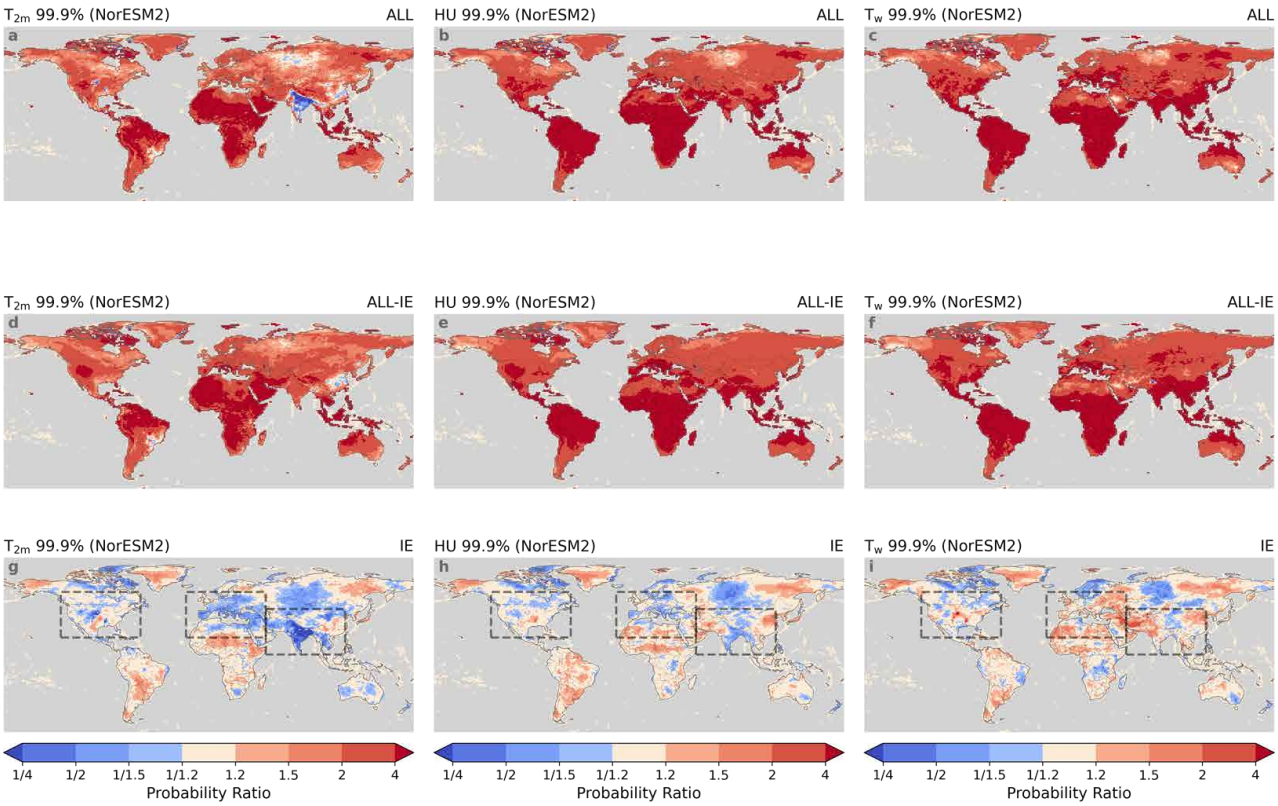
Supplementary Figure S21 | Same as Figure S16 but calculated based on CNRM-CM6-1 outputs.



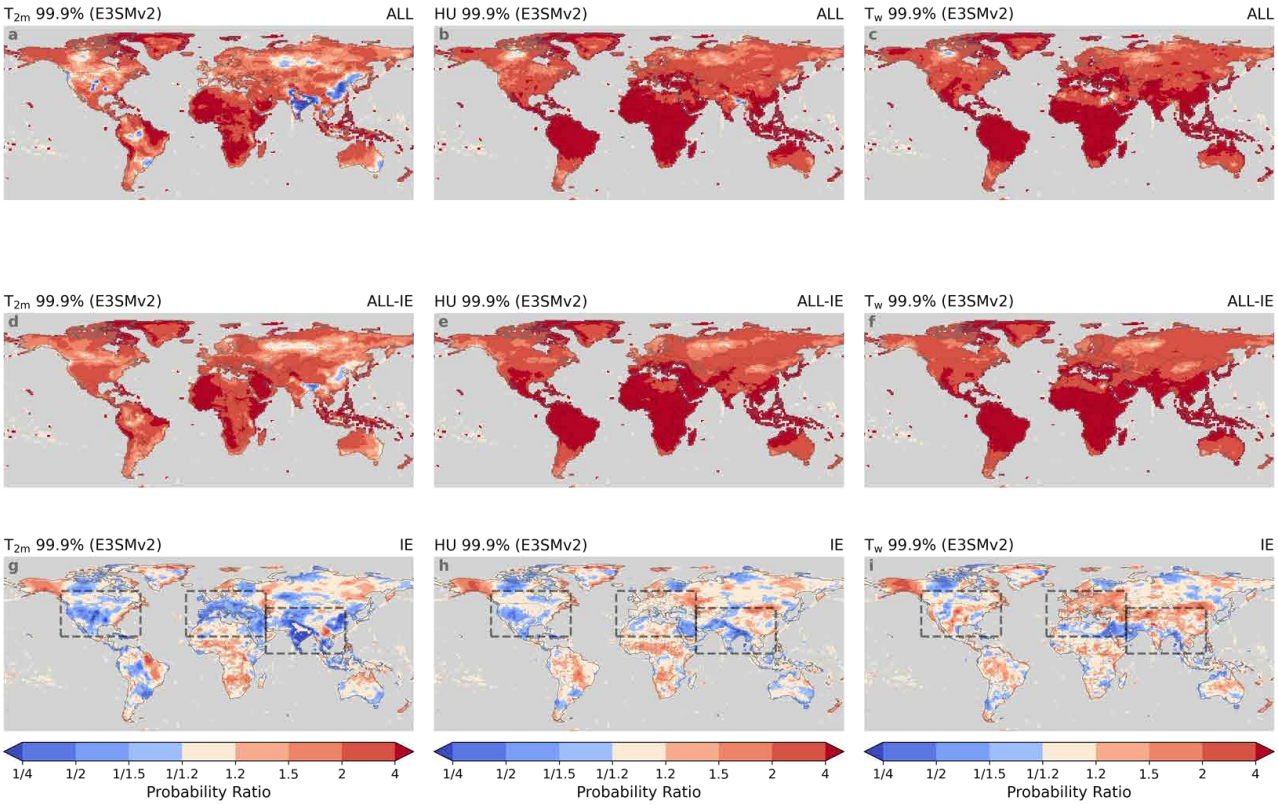
Supplementary Figure S22 | Impacts of different forcings on frequency of 2-meter air temperature, HUMIDEX, and wet-bulb temperature extreme event as simulated by CESM2. a-i Impacts of all forcings (ALL: **a, b, c**), all forcings except irrigation expansion (ALL-IE: **d, e, f**), and irrigation expansion (IE) on the frequency of the events in which 2-meter air temperature (T_{2m}: **a, d, g**), HUMIDEX (HU: **b, e, h**), and wet bulb temperature (T_w: **c, f, i**) exceed their 99.9th percentile values of the first 30 years (1901-1930) in the simulations without irrigation expansion (*1901irr*). Impacts are quantified by probability ratio (PR) which is calculated by dividing the events frequencies in the new exp_period by those in the reference exp_period (see Table 1 in main text), and the values are calculated based on CESM2 outputs.



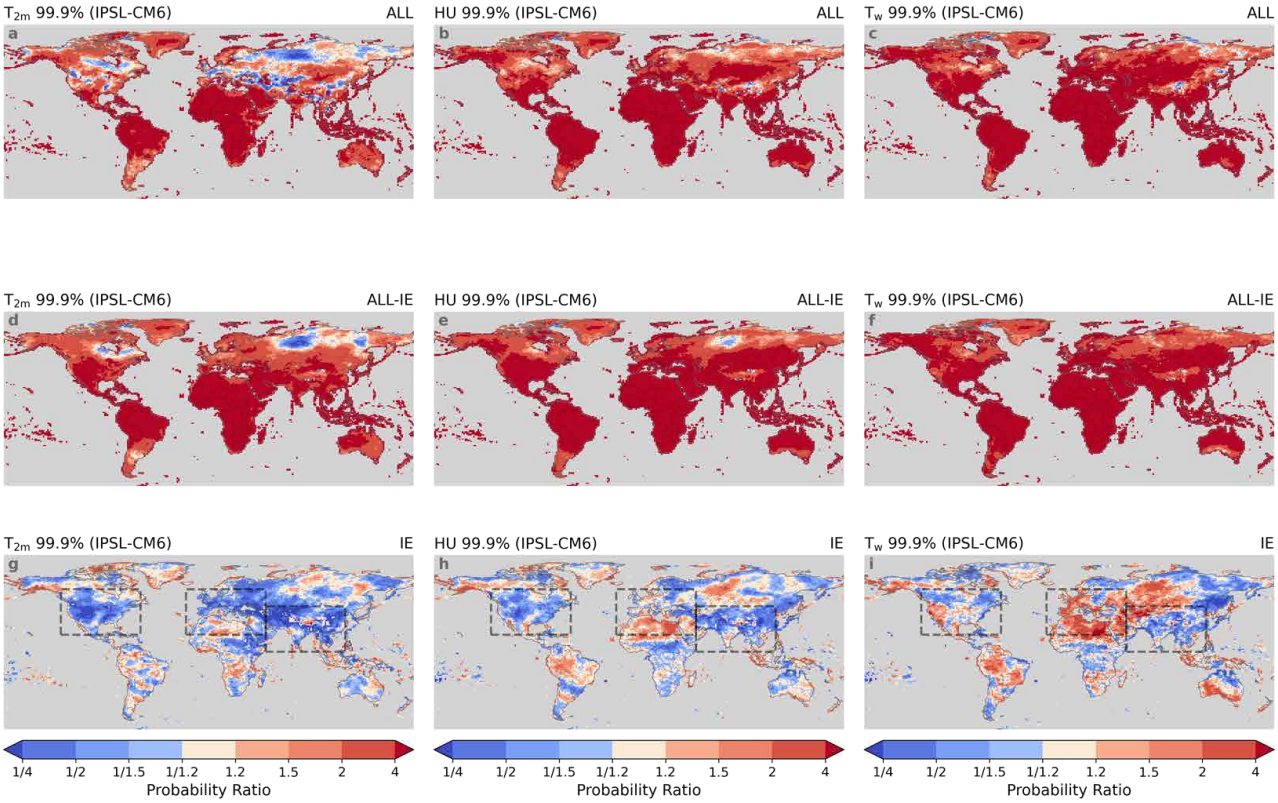
Supplementary Figure S23 | Same as Figure S22 but calculated based on CESM2_gw outputs.



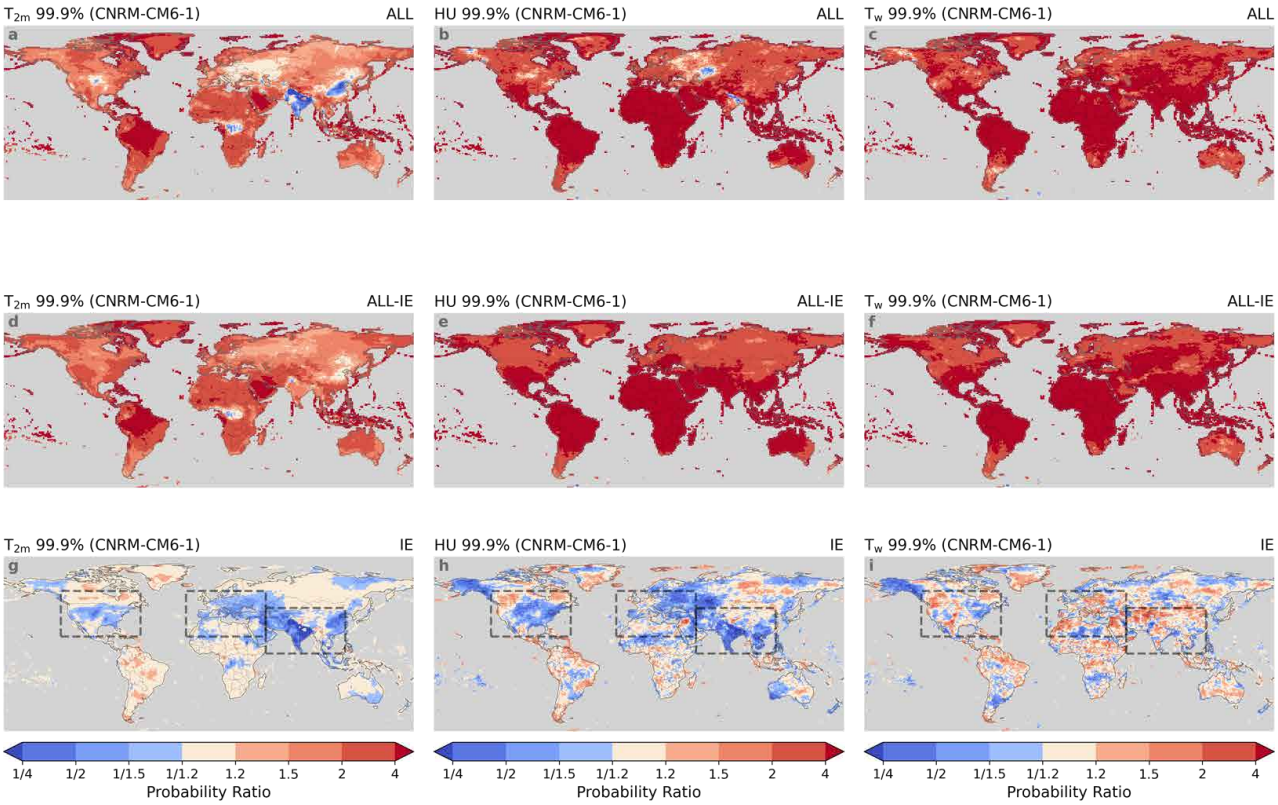
Supplementary Figure S24 | Same as Figure S22 but calculated based on NorESM2 outputs.



Supplementary Figure S25 | Same as Figure S22 but calculated based on E3SMv2 outputs.

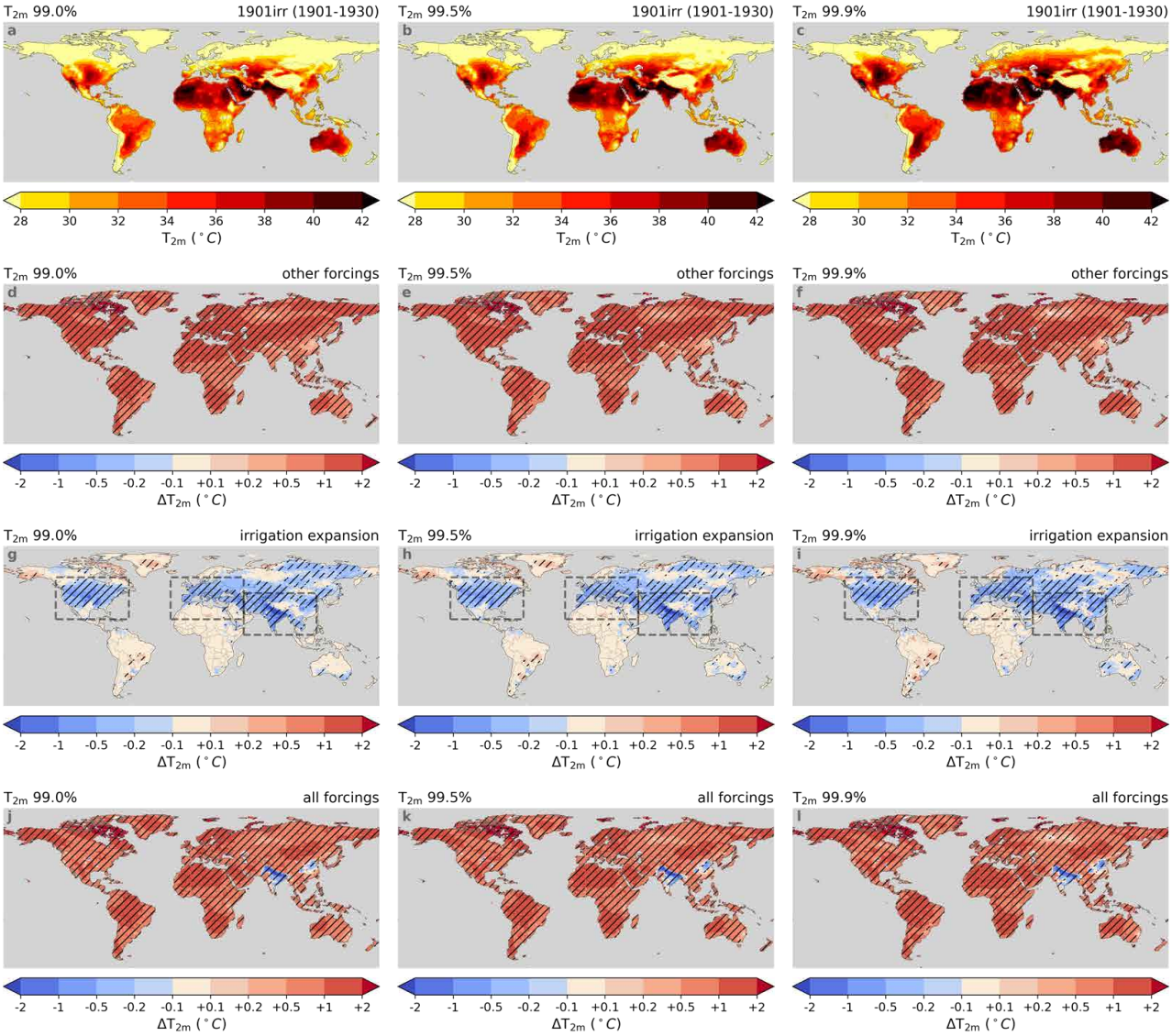


Supplementary Figure S26 | Same as Figure S22 but calculated based on IPSL-CM6 outputs.

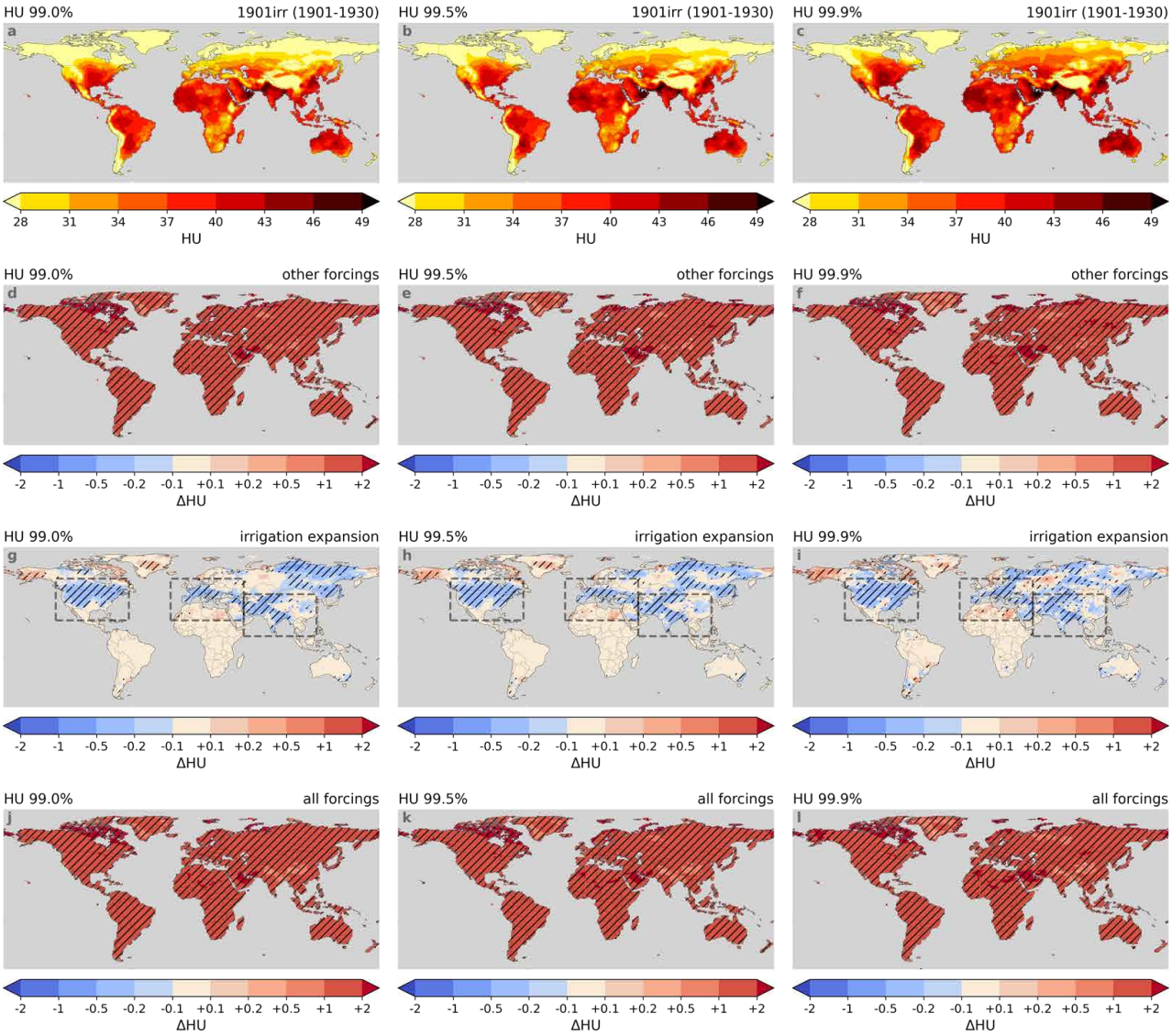


Supplementary Figure S27 | Same as Figure S22 but calculated based on CNRM-CM6-1 outputs.

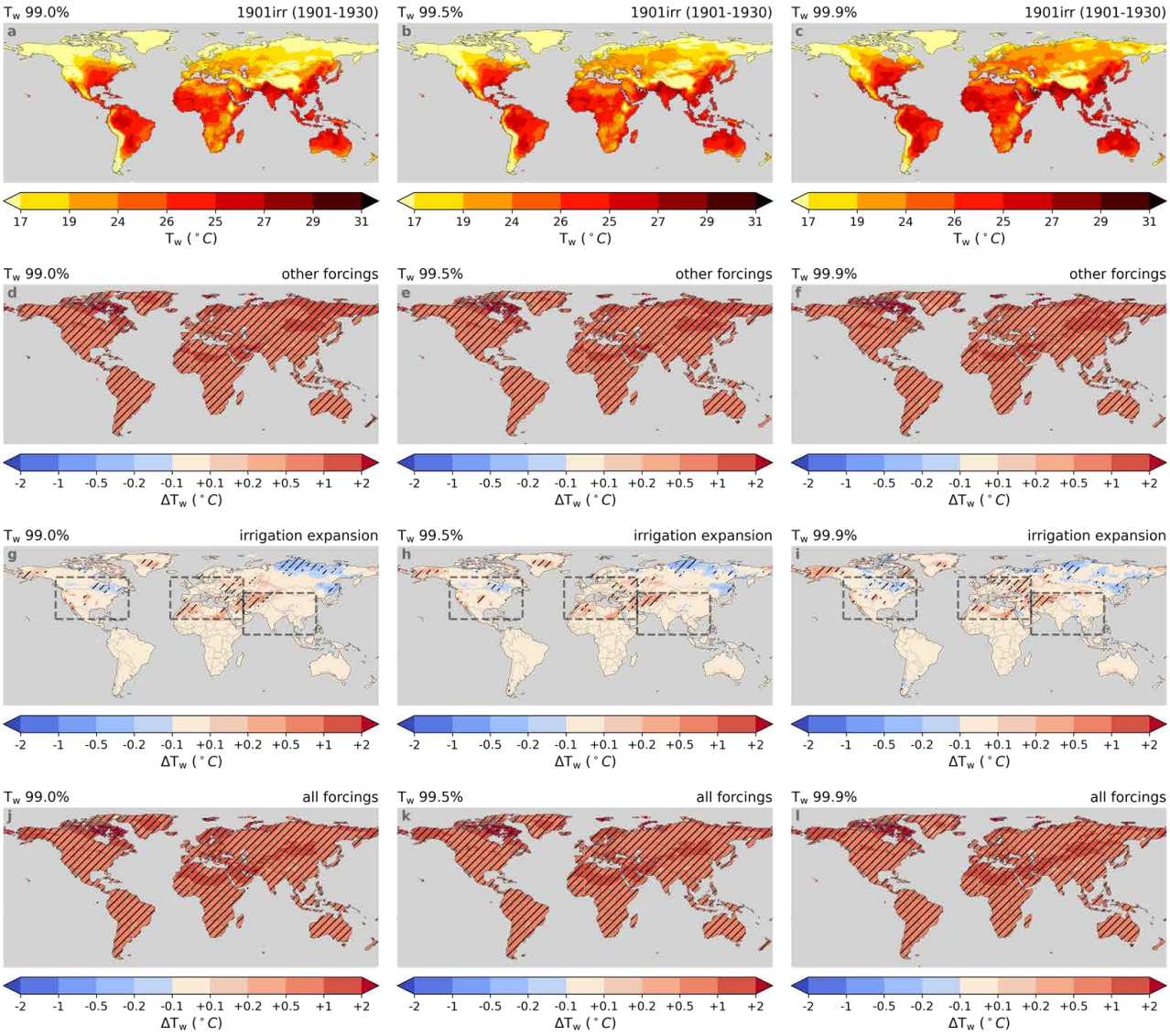
2.3 Supplementary Figures 3: Results of individual metrics



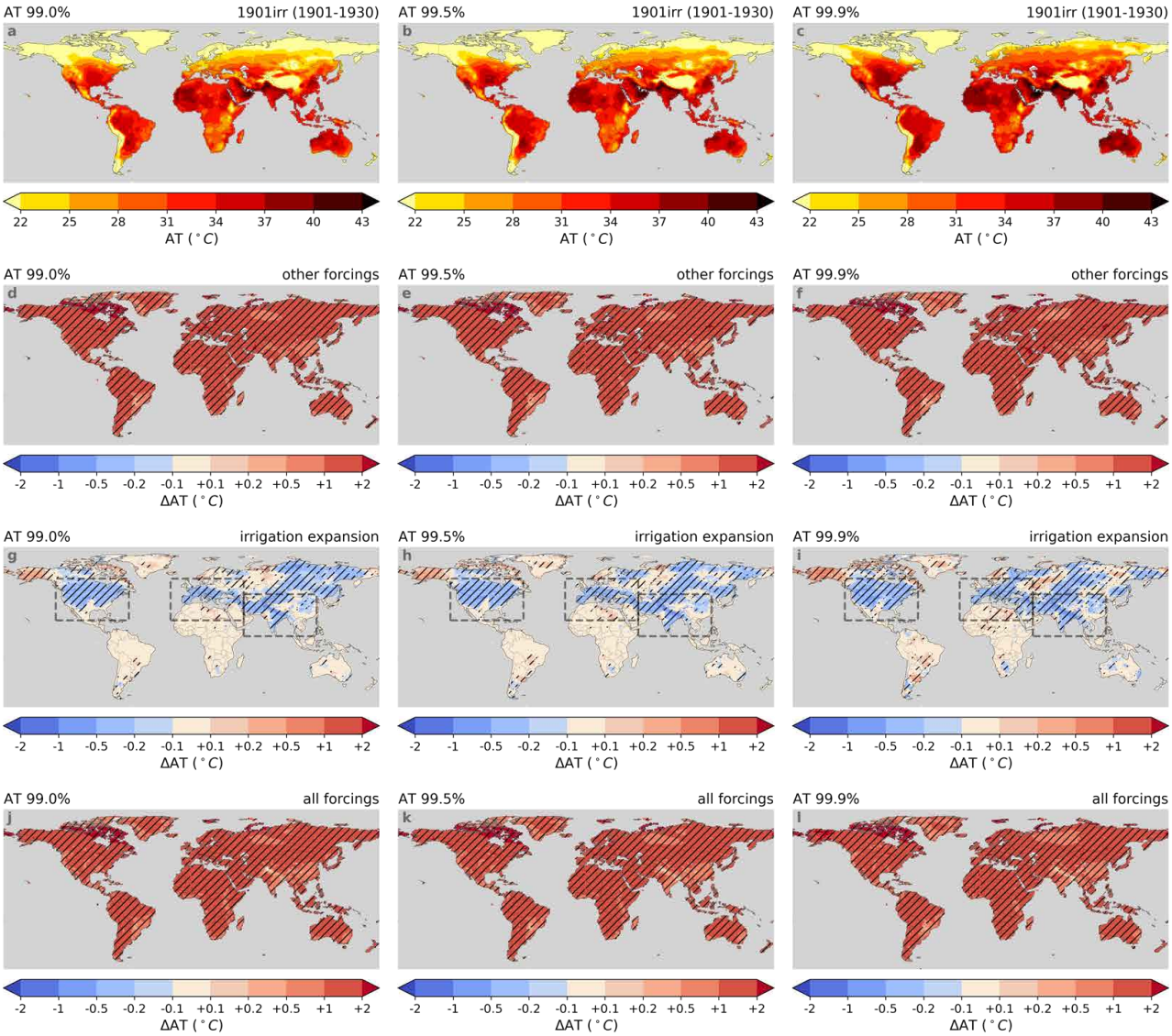
Supplementary Figure S28 | **a-c** Multi-model mean absolute values of the 99th (**a**), 99.5th (**b**), and 99.9th (**c**) percentile values of 2-meter air temperature (T_{2m}) of the first 30 years (1901-1930) in the simulations without irrigation expansion (*1901irr*). **d-l** Multi-model mean impacts of all forcings (ALL: greenhouse gas emissions, land use and land management change, irrigation expansion, etc.) (**d, e, f**), all forcings except irrigation expansion (ALL-IE: **g, h, i**), and irrigation expansion (IE: **j, k, l**) on the 99th, 99.5th, and 99.9th percentile values of T_{2m} (**d, g, j**), HU (**e, h, k**), and T_w (**f, i, l**). Impacts are calculated by subtracting the values in the new exp_period by those in the reference exp_period (see Table 1 in main text). Only signals (>0.1 or <-0.1) agreed by $\geq$ 5 of 6 models are shown.



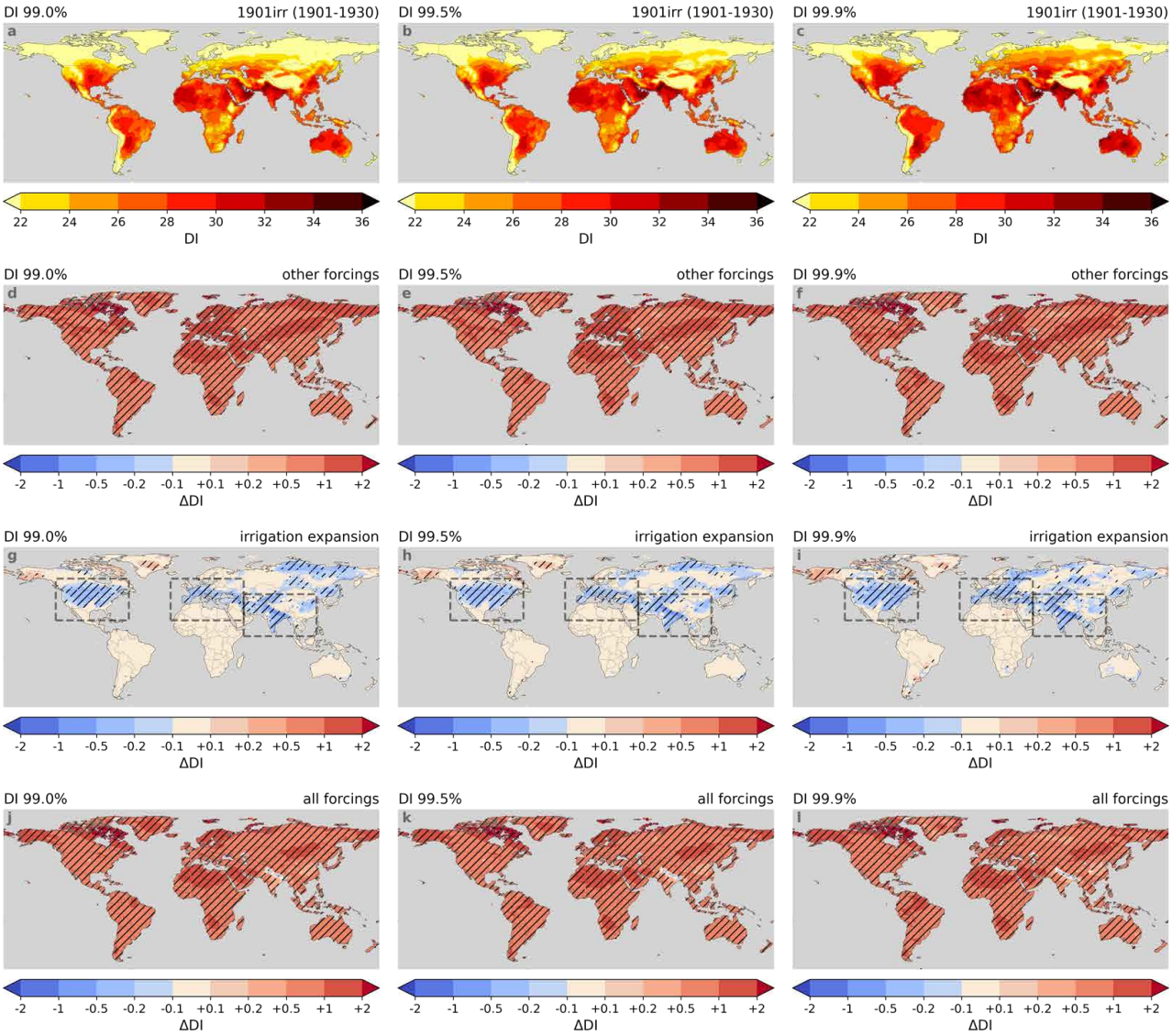
Supplementary Figure S29 | Same as Figure S28 bu for HUMIDEX (HU).



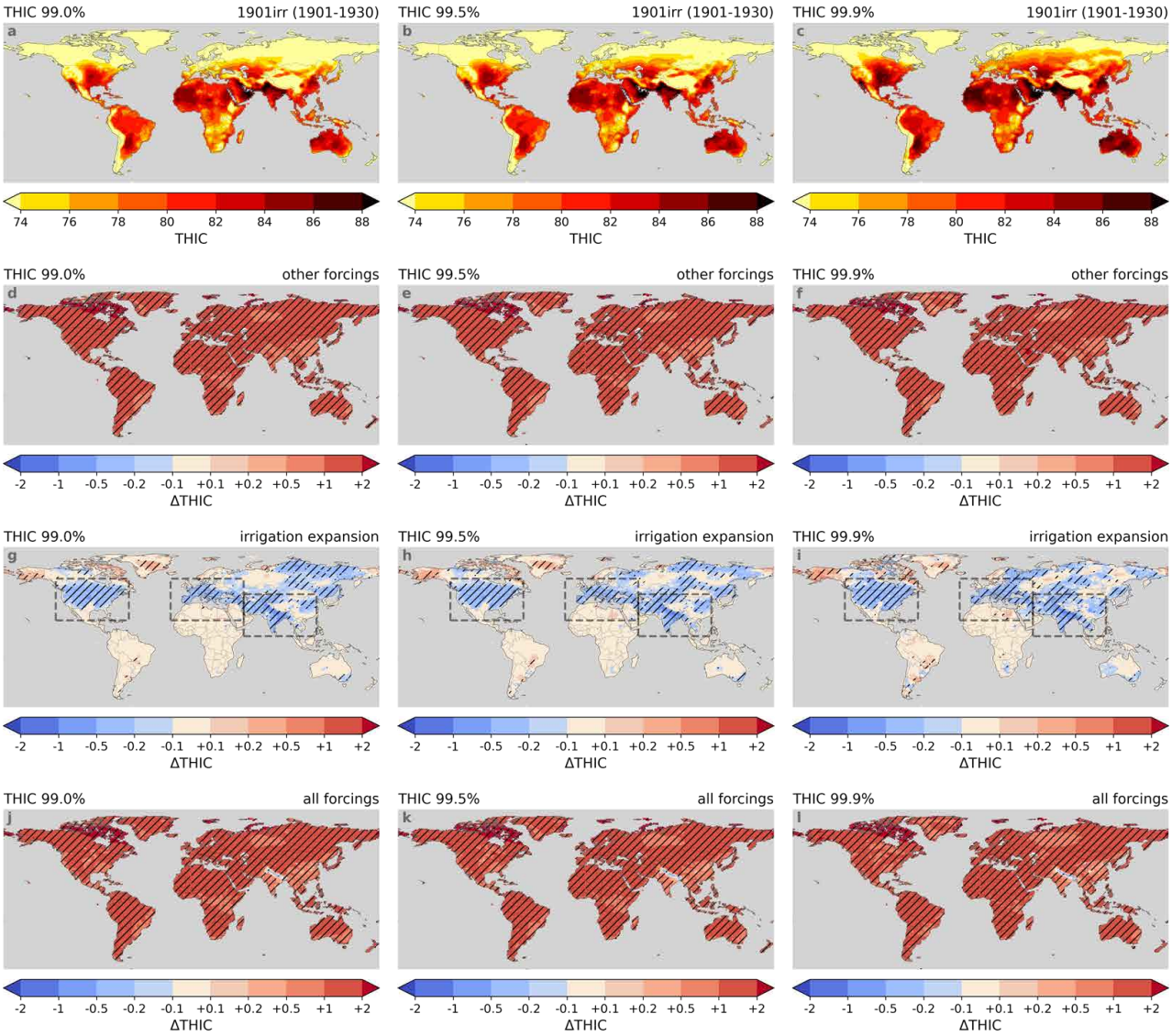
Supplementary Figure S30 | Same as Figure S28 bu for wet-bulb temperature (T_w).



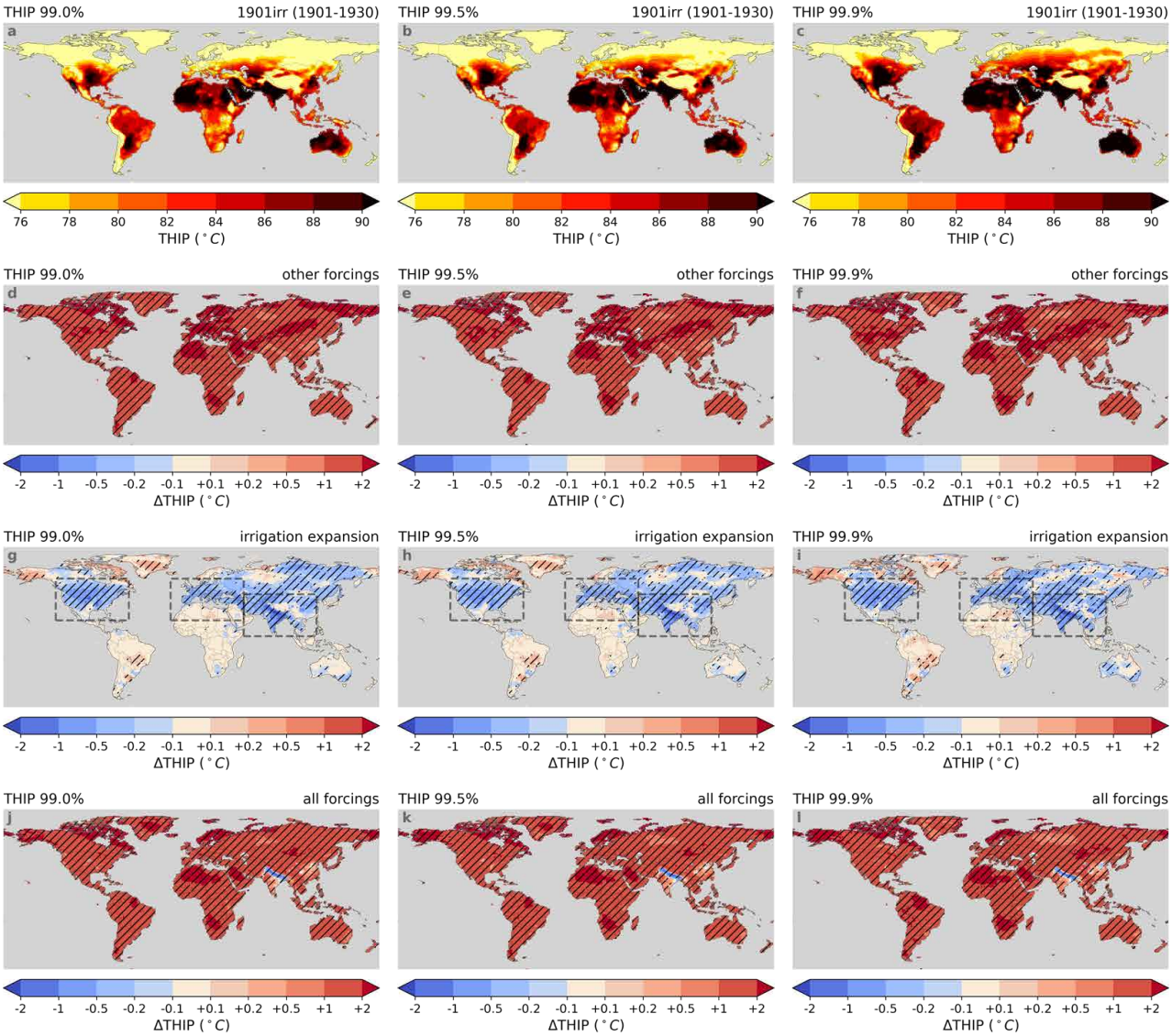
Supplementary Figure S31 | Same as Figure S28 bu for Apparent Temperature (AT). The only difference is that AT is only calculated based on outputs from five models (except CNRM-CM6-1).



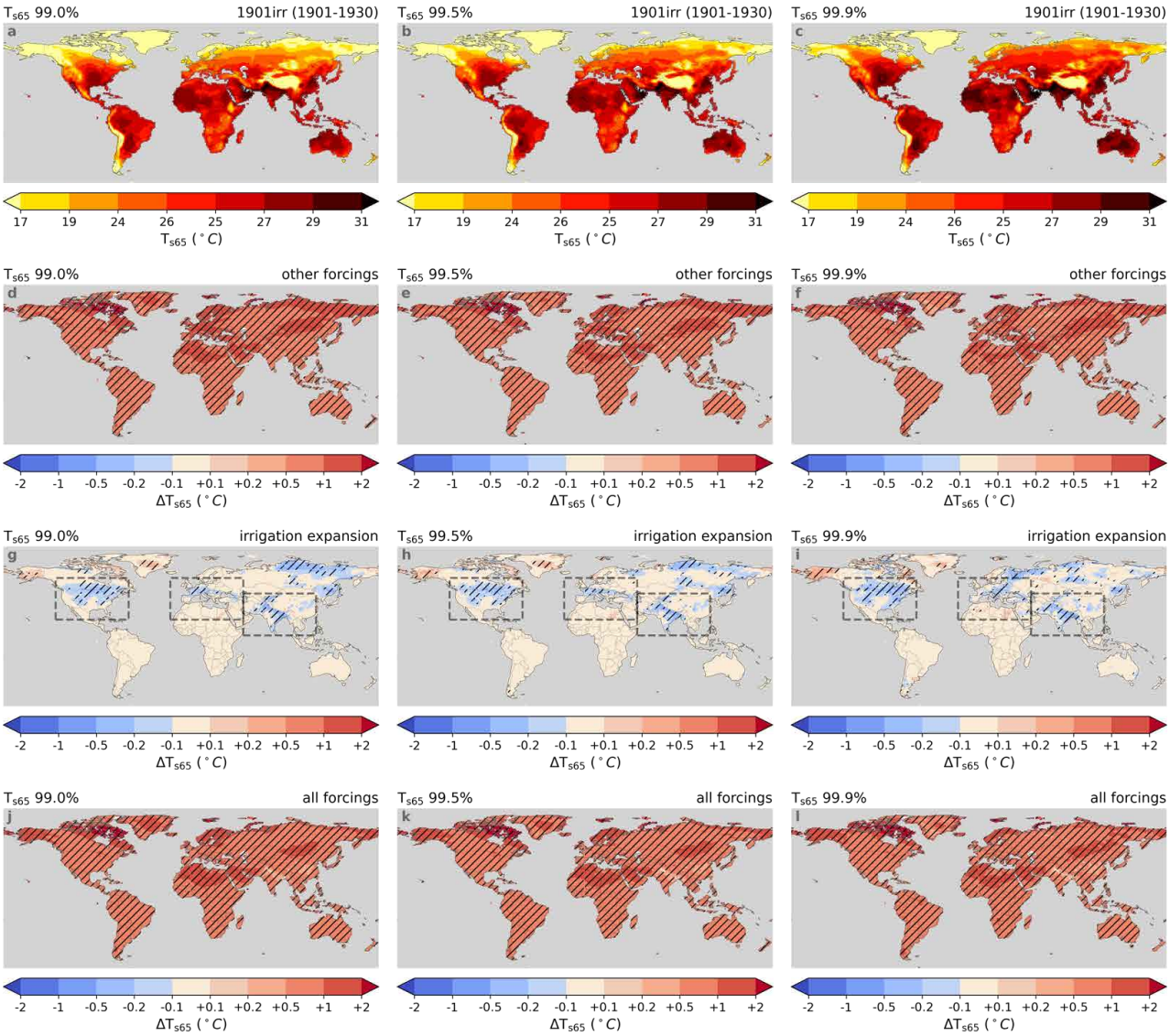
Supplementary Figure S32 | Same as Figure S28 bu for Discomfort Index (DI).



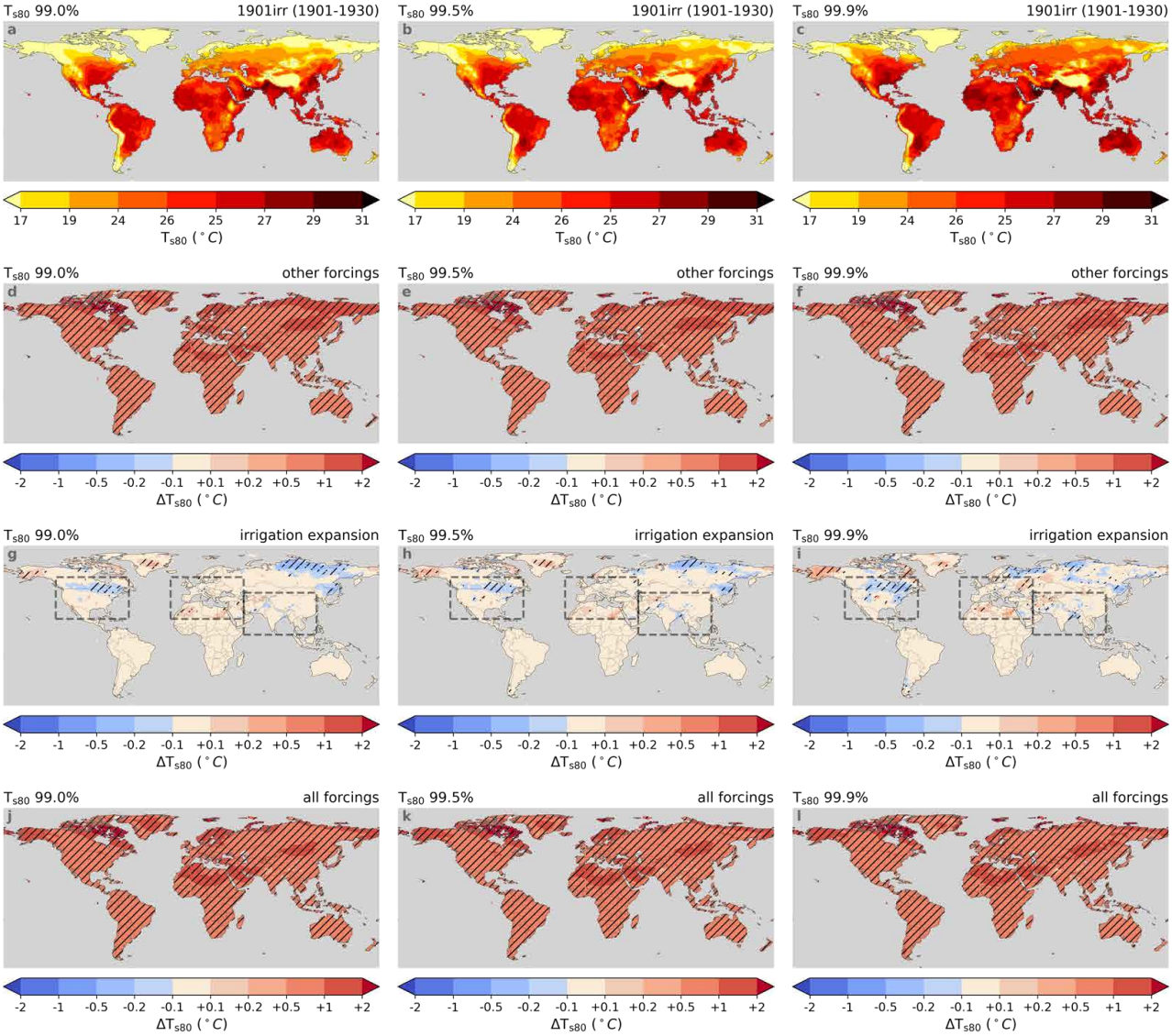
Supplementary Figure S33 | Same as Figure S28 bu for Temperature Humidity Index for Comfort (THIC).



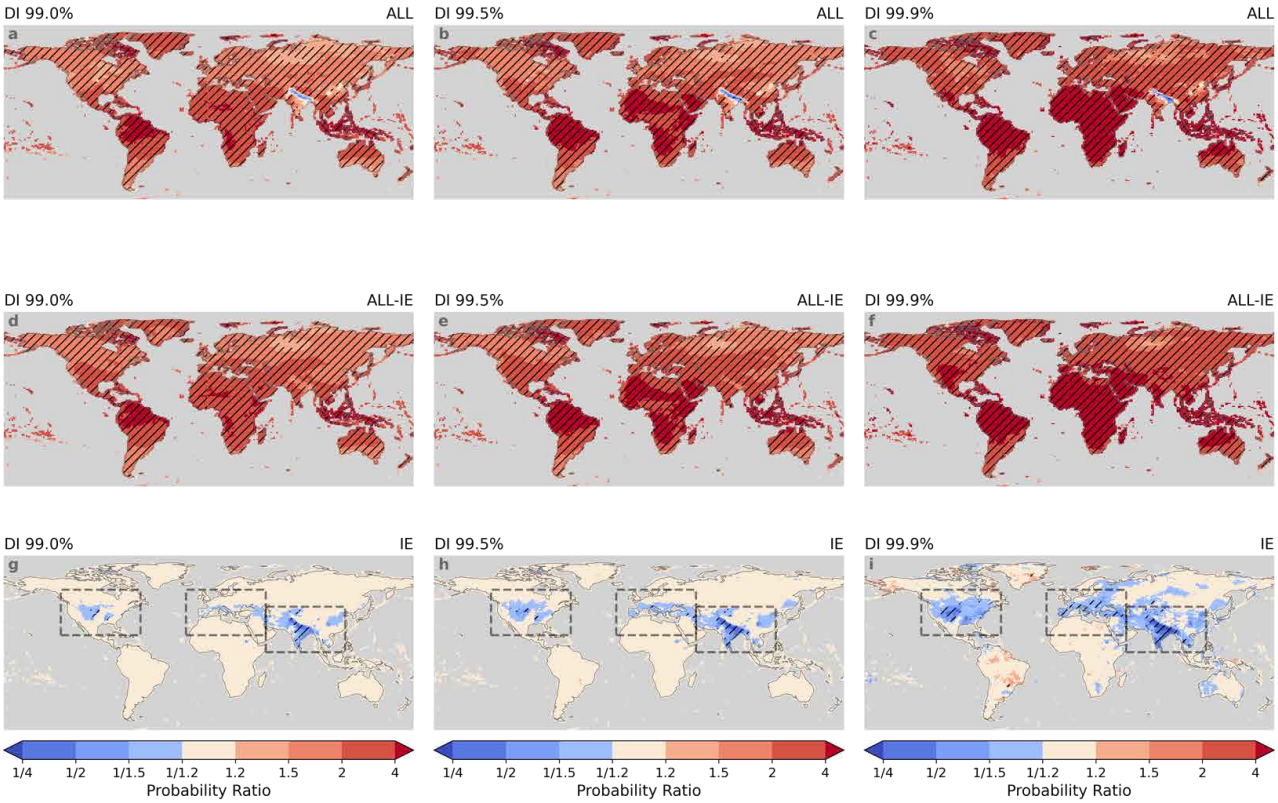
Supplementary Figure S34 | Same as Figure S28 bu for Temperature Humidity Index for Physiology (THIP).



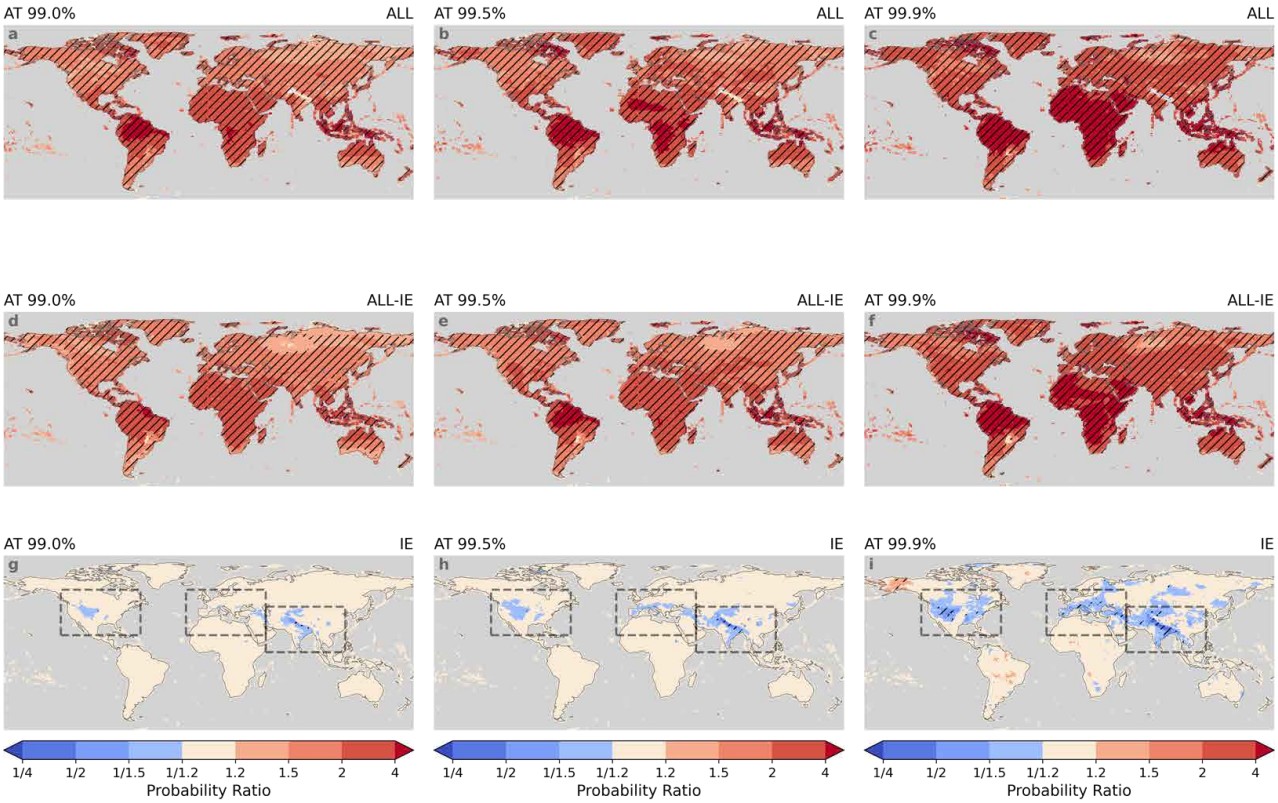
Supplementary Figure S35 | Same as Figure S28 bu for the temperature when 65% of the swamp coolers are approached (T_{s65}).



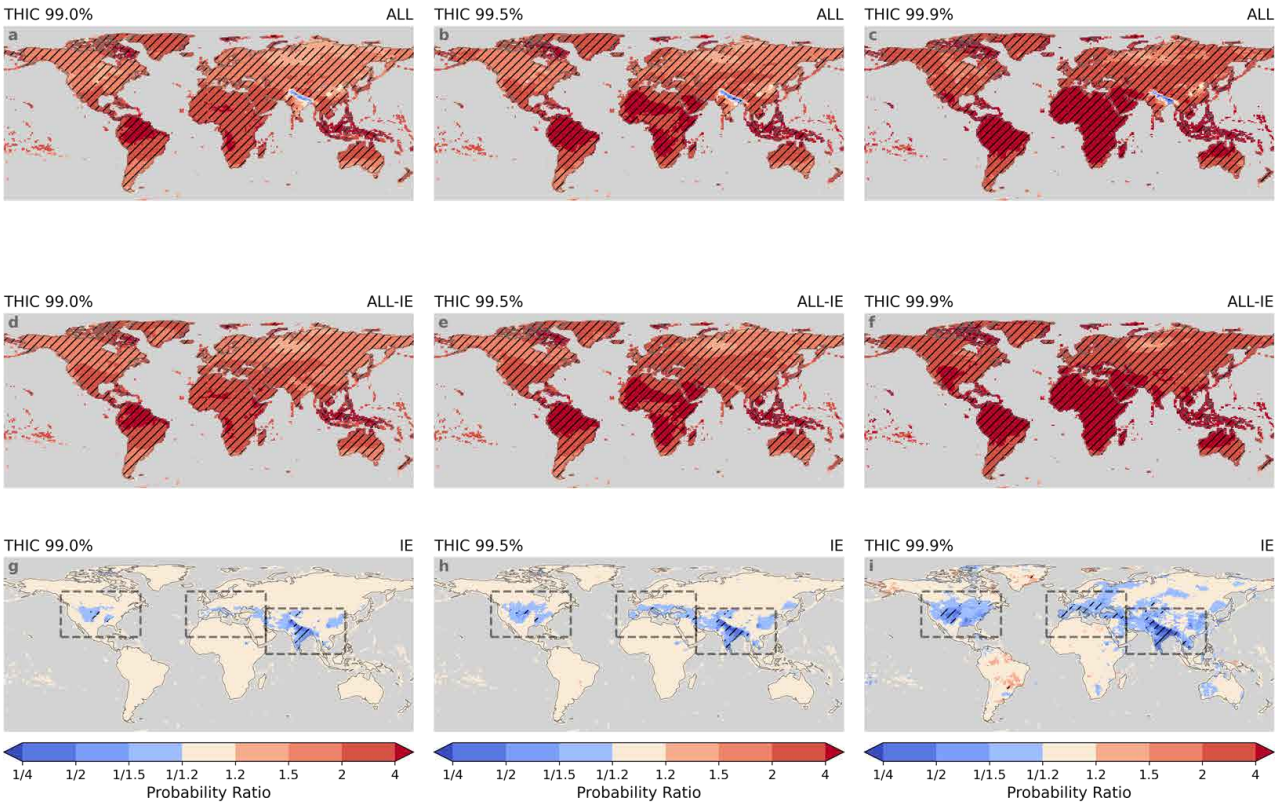
Supplementary Figure S36 | Same as Figure S28 bu for the temperature when 80% of the swamp coolers are approached (T_{s80}).



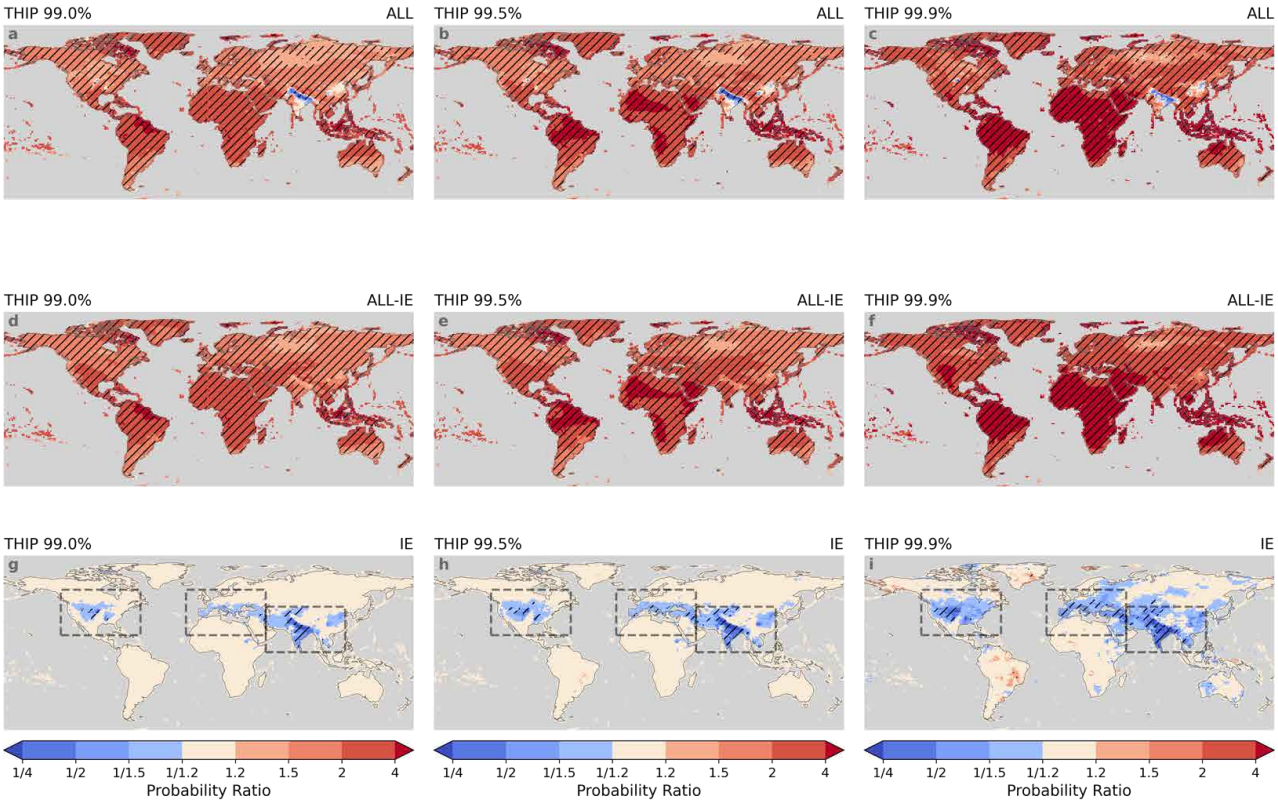
Supplementary Figure S37 | **a-i** Impacts of all forcings (ALL: **a, b, c**), all forcings except irrigation expansion (ALL-IE: **d, e, f**), and irrigation expansion (IE) on the frequency of the events in which Discomfort Index (DI) exceed its 99$^{\text{th}}$ (**a, d, g**), 99.5$^{\text{th}}$ (**b, e, h**), and 99.9$^{\text{th}}$ (**c, f, i**) percentile values of the first 30 years (1901-1930) in the simulations without irrigation expansion (*1901irr*) shown in Figure S32**a-c**. Impacts are quantified by probability ratio (PR) which is calculated by dividing the events frequencies in the new exp_period by those in the reference exp_period (see Table 1 in main text), and the values are the sixth root of the product of PR calculated from the outputs of six ESMs. Only signals (>1.2 or <1/1.2) agreed by $\geq$ 5 of 6 models are shown.



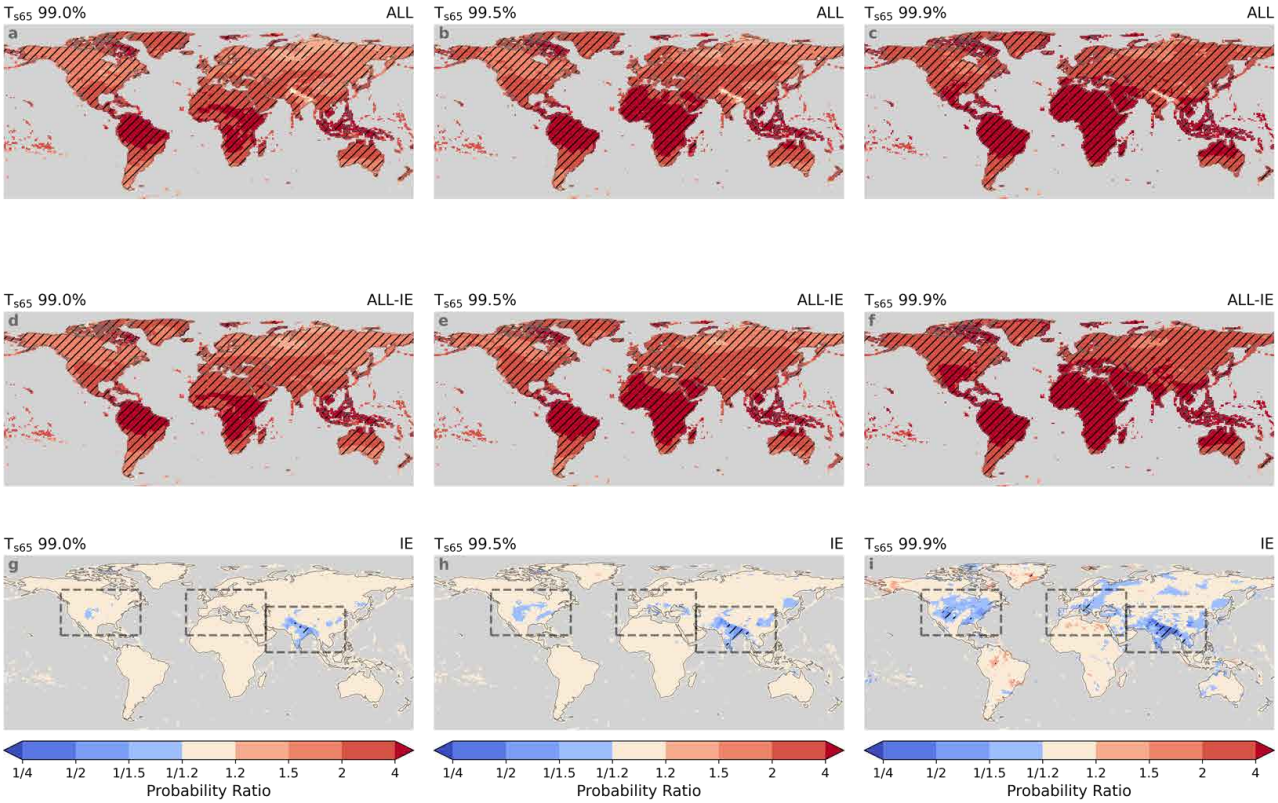
Supplementary Figure S38 | Same as Figure S37 bu for Apparent Temperature (AT). The only difference is that AT is only calculated based on outputs from five models (except CNRM-CM6-1).



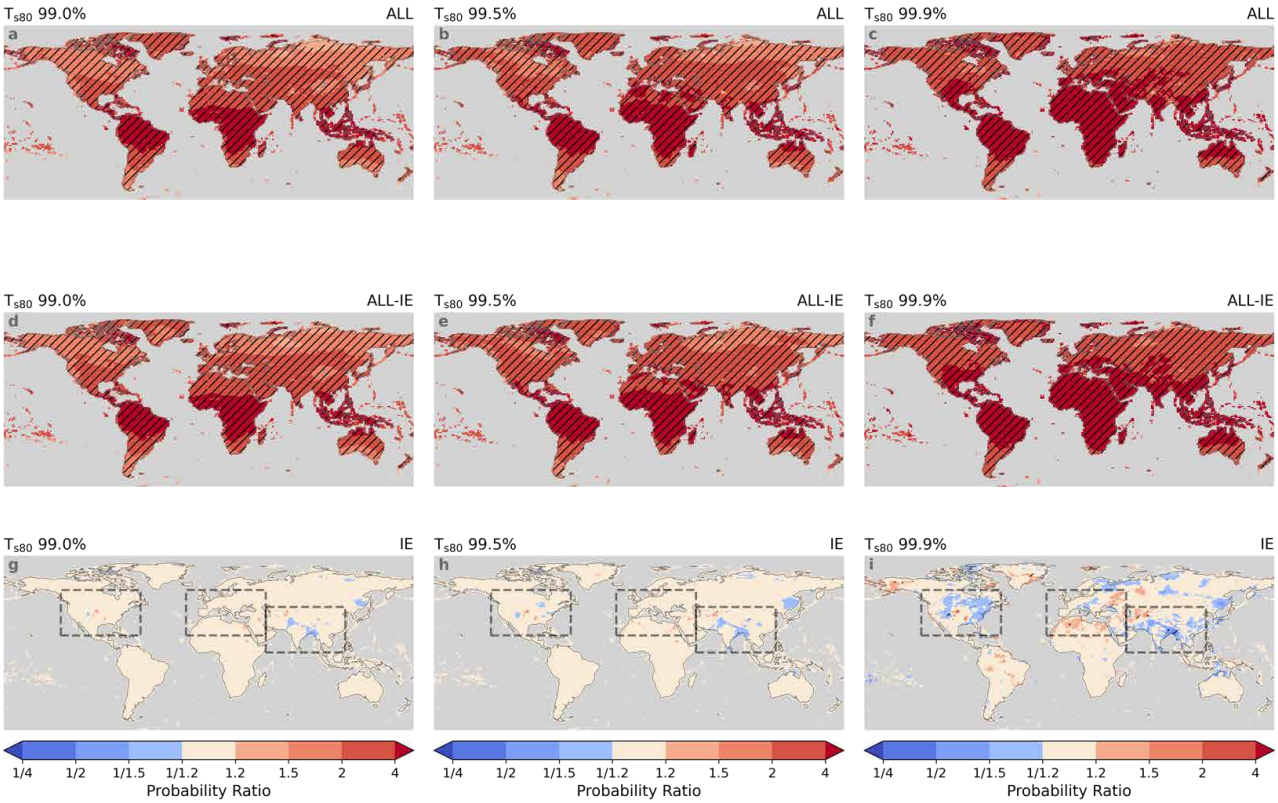
Supplementary Figure S39 | Same as Figure S37 bu for Temperature Humidity Index for Comfort (THIC).



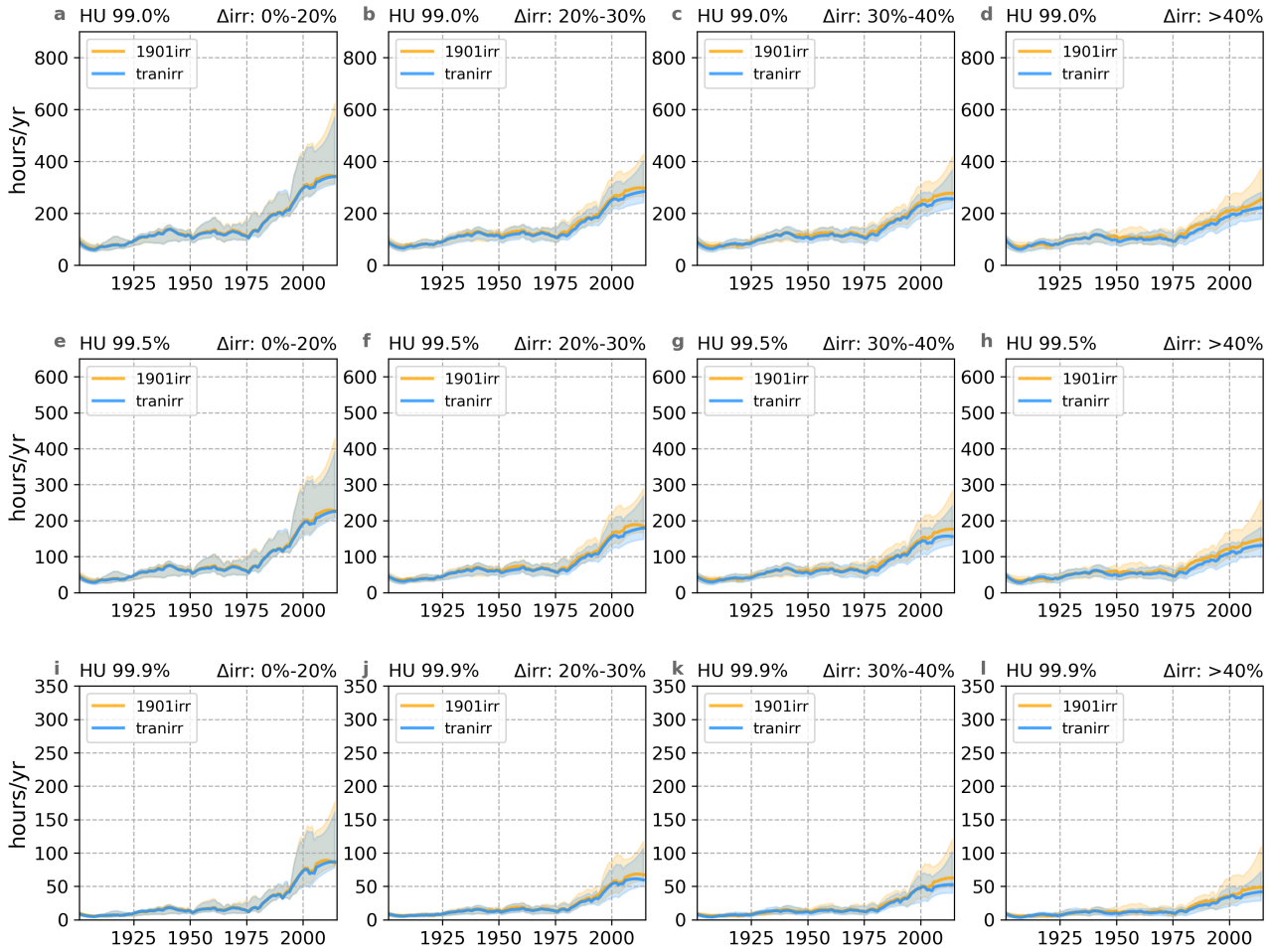
Supplementary Figure S40 | Same as Figure S37 bu for Temperature Humidity Index for Physiology (THIP).



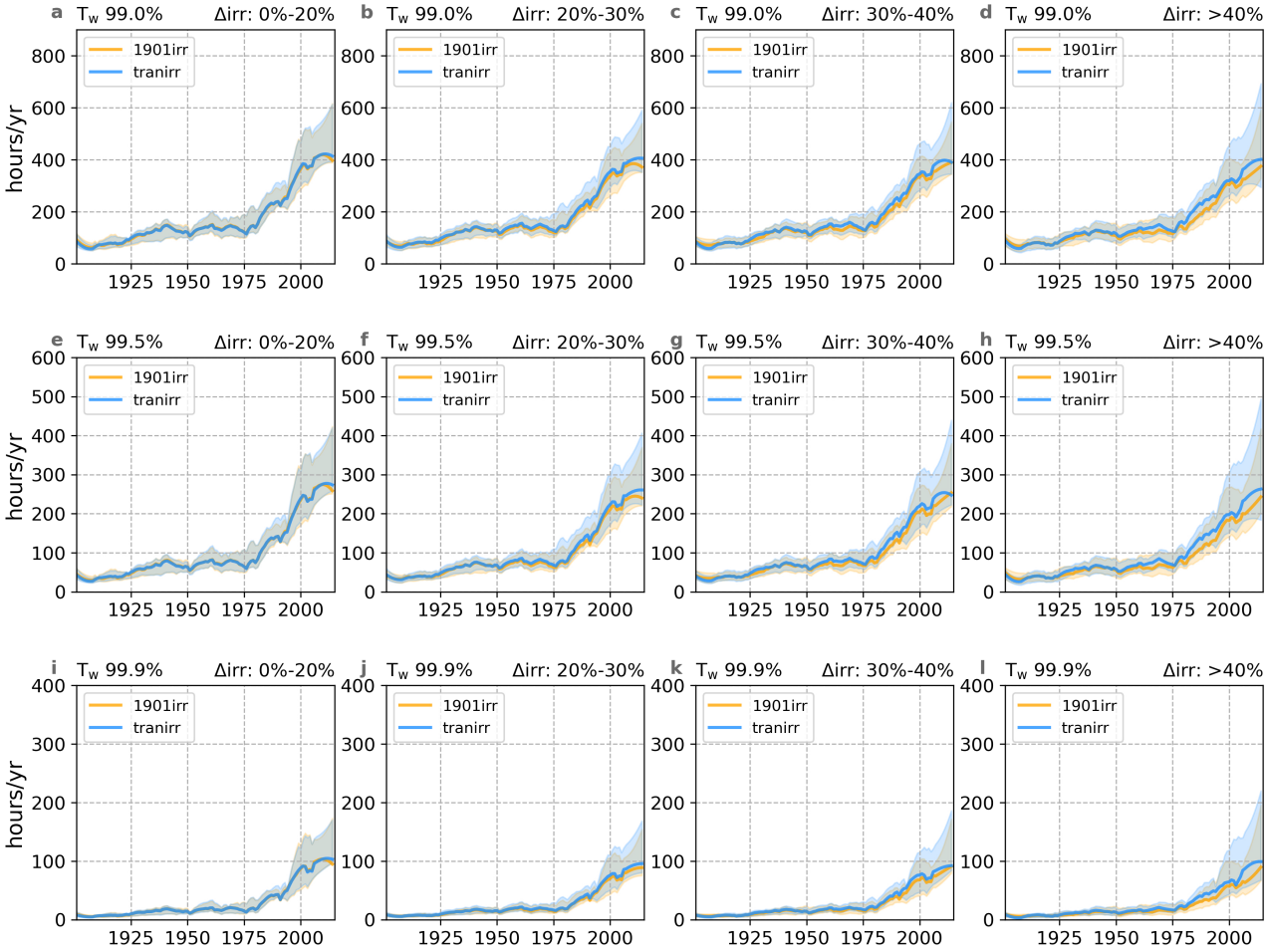
Supplementary Figure S41 | Same as Figure S37 bu for the temperature when 65% of the swamp coolers are approached (T_{s65}).



Supplementary Figure S42 | Same as Figure S37 bu for the temperature when 80% of the swamp coolers are approached (T_{s80}).



Supplementary Figure S43 | Time series of the annual hours over the grid cells with 0-20% (**a, e, i**), 20%-30% (**b, f, j**), 30%-40% (**c, g, k**) and >40% (**d, h, i**) of irrigated fraction increase (in the year 2014 compared to the year 1901) of HUMIDEX warm extremes. The warm extremes are defined as the period when HU exceed their 99^{th} (**a-d**), 99.5^{th} (**e-h**), and 99.9^{th} (**i-l**) percentile values of the first 30 years (1901-1930) in the simulations without irrigation expansion (*1901irr*). Lines indicate the median value among six models and ranges indicate the 25$\hat{\text{th}}$ and 75$\hat{\text{th}}$ percentile values of six models outputs. Curves were smoothed using Savitzky-Golay filtering (order = 2, window = 15)[1]. The range of the y-axes are different for three sub-plots.



Supplementary Figure S44 | Same as Figure S43 but for wet-bulb temperature (T_w).

Supplementary References

[1] Savitzky, A. & Golay, M. Smoothing and differentiation of data by simplified least squares procedures.. *Analytical Chemistry*. **36**, 1627-1639 (1964)

[2] Bogenschutz, P., Gettelman, A., Hannay, C., Larson, V., Neale, R., Craig, C. & Chen, C. The path to CAM6: Coupled simulations with CAM5. 4 and CAM5. 5. *Geoscientific Model Development*. **11**, 235-255 (2018)

[3] Lawrence, D., Fisher, R., Koven, C., Oleson, K., Swenson, S., Bonan, G., Collier, N., Ghimire, B., Kampenhout, L., Kennedy, D. & Others The Community Land Model version 5: Description of new features, benchmarking, and impact of forcing uncertainty. *Journal Of Advances In Modeling Earth Systems*. **11**, 4245-4287 (2019)

[4] Danabasoglu, G., Lamarque, J., Bacmeister, J., Bailey, D., DuVivier, A., Edwards, J., Emmons, L., Fasullo, J., Garcia, R., Gettelman, A. & Others The community earth system model version 2 (CESM2). *Journal Of Advances In Modeling Earth Systems*. **12**, e2019MS001916 (2020)

[5] Li, H., Wigmosta, M., Wu, H., Huang, M., Ke, Y., Coleman, A. & Leung, L. A physically based runoff routing model for land surface and earth system models. *Journal Of Hydrometeorology*. **14**, 808-828 (2013)

[6] Li, H., Leung, L., Getirana, A., Huang, M., Wu, H., Xu, Y., Guo, J. & Voisin, N. Evaluating global streamflow simulations by a physically based routing model coupled with the community land model. *Journal Of Hydrometeorology*. **16**, 948-971 (2015)

[7] Zhu, B., Huang, M., Cheng, Y., Xie, X., Liu, Y., Zhang, X., Bisht, G., Chen, X., Missik, J. & Liu, H. Effects of irrigation on water, carbon, and nitrogen budgets in a semiarid watershed in the Pacific northwest: A modeling study. *Journal Of Advances In Modeling Earth Systems*. **12**, e2019MS001953 (2020)

[8] Yao, Y., Vanderkelen, I., Lombardozzi, D., Swenson, S., Lawrence, D., Jägermeyr, J., Grant, L. & Thiery, W. Implementation and evaluation of irrigation techniques in the community land model. *Journal Of Advances In Modeling Earth Systems*. **14**, e2022MS003074 (2022)

[9] Felfelani, F., Lawrence, D. & Pokhrel, Y. Representing intercell lateral groundwater flow and aquifer pumping in the community land model. *Water Resources Research*. **57**, e2020WR027531 (2021)

[10] Seland, Ø., Bentsen, M., Olivié, D., Toniazzo, T., Gjermundsen, A., Graff, L., Debernard, J., Gupta, A., He, Y., Kirkevåg, A. & Others Overview of the Norwegian Earth System Model (NorESM2) and key climate response of CMIP6 DECK, historical, and scenario simulations. *Geoscientific Model Development*. **13**, 6165-6200 (2020)

[11] Kirkevåg, A., Grini, A., Olivié, D., Seland, Ø., Alterskjær, K., Hummel, M., Karset, I., Lewinschal, A., Liu, X., Makkonen, R. & Others A production-tagged aerosol module for Earth system models, OsloAero5. 3–extensions and updates for CAM5. 3-Oslo. *Geoscientific Model Development*. **11**, 3945-3982 (2018)

[12] Toniazzo, T., Bentsen, M., Craig, C., Eaton, B., Edwards, J., Goldhaber, S., Jablonowski, C. & Lauritzen, P. Enforcing conservation of axial angular momentum in the atmospheric general circulation model CAM6. *Geoscientific Model Development*. **13**, 685-705 (2020)

[13] Golaz, J., Caldwell, P., Van Roekel, L., Petersen, M., Tang, Q., Wolfe, J., Abeshu, G., Anantharaj, V., Asay-Davis, X., Bader, D. & Others The DOE E3SM coupled model version 1: Overview and evaluation at standard resolution. *Journal Of Advances In Modeling Earth Systems*. **11**, 2089-2129 (2019)

[14] Golaz, J., Van Roekel, L., Zheng, X., Roberts, A., Wolfe, J., Lin, W., Bradley, A., Tang, Q., Maltrud, M., Forsyth, R. & Others The DOE E3SM Model Version 2: Overview of the physical model and initial model evaluation. *Journal Of Advances In Modeling Earth Systems*. **14**, e2022MS003156 (2022)

[15] Leung, L., Bader, D., Taylor, M. & McCoy, R. An introduction to the E3SM special collection: Goals, science drivers, development, and analysis. *Journal Of Advances In Modeling Earth Systems*. **12**, e2019MS001821 (2020)

[16] Zhou, T., Leung, L., Leng, G., Voisin, N., Li, H., Craig, A., Tesfa, T. & Mao, Y. Global irrigation characteristics and effects simulated by fully coupled land surface, river, and water management models in E3SM. *Journal Of Advances In Modeling Earth Systems*. **12**, e2020MS002069 (2020)

[17] Leng, G., Leung, L. & Huang, M. Significant impacts of irrigation water sources and methods on modeling irrigation effects in the ACME L and Model. *Journal Of Advances In Modeling Earth Systems*. **9**, 1665-1683 (2017)

[18] Hourdin, F., Rio, C., Grandpeix, J., Madeleine, J., Cheruy, F., Rochetin, N., Jam, A., Musat, I., Idelkadi, A., Fairhead, L. & Others LMDZ6A: The atmospheric component of the IPSL climate model with improved and better tuned physics. *Journal Of Advances In Modeling Earth Systems*. **12**, e2019MS001892 (2020)

[19] Boucher, O., Servonnat, J., Albright, A., Aumont, O., Balkanski, Y., Bastrikov, V., Bekki, S., Bonnet, R., Bony, S., Bopp, L. & Others Presentation and evaluation of the IPSL-CM6A-LR climate model. *Journal Of Advances In Modeling Earth Systems*. **12**, e2019MS002010 (2020)

[20] Arboleda-Obando, P., Ducharne, A., Yin, Z. & Ciais, P. Validation of a new global irrigation scheme in the land surface model ORCHIDEE v2. 2. *Geoscientific Model Development*. **17**, 2141-2164 (2024)

[21] Siebert, S., Burke, J., Faures, J., Frenken, K., Hoogeveen, J., Döll, P. & Portmann, F. Groundwater use for irrigation–a global inventory. *Hydrology And Earth System Sciences*. **14**, 1863-1880 (2010)

[22] Wisser, D., Fekete, B., Vörösmarty, C. & Schumann, A. Reconstructing 20th century global hydrography: a contribution to the Global Terrestrial Network-Hydrology (GTN-H). *Hydrology And Earth System Sciences*. **14**, 1-24 (2010)

[23] Gates, W., Boyle, J., Covey, C., Dease, C., Doutriaux, C., Drach, R., Fiorino, M., Gleckler, P., Hnilo, J., Marlais, S. & Others An overview of the results of the Atmospheric Model Intercomparison Project (AMIP I). *Bulletin Of The American Meteorological Society*. **80**, 29-56 (1999)

[24] Hurtt, G., Chini, L., Sahajpal, R., Frolking, S., Bodirsky, B., Calvin, K., Doelman, J., Fisk, J., Fujimori, S., Klein Goldewijk, K. & Others Harmonization of global land use change and management for the period 850–2100 (LUH2) for CMIP6. *Geoscientific Model Development*. **13**, 5425-5464 (2020)

[25] Steadman, R. A universal scale of apparent temperature. *Journal Of Applied Meteorology And Climatology*. **23**, 1674-1687 (1984)

[26] Steadman, R. Norms of apparent temperature in Australia. *Aust. Met. Mag.* **43** pp. 1-16 (1994)

[27] NWSCR, Livestock Hot Weather Stress: Regional Operations Manual Letter. (NWSCR (National Weather Service Central Region) Kansas City, MO, USA,1976)

[28] Ingram, D. Evaporative cooling in the pig. *Nature*. **207**, 415-416 (1965)

[29] Thom, E. The discomfort index. *Weatherwise*. **12**, 57-61 (1959)

[30] Epstein, Y. & Moran, D. Thermal comfort and the heat stress indices. *Industrial Health*. **44**, 388-398 (2006)

[31] Giles, B., Balafoutis, C. & Maheras, P. Too hot for comfort: the heatwaves in Greece in 1987 and 1988. *International Journal Of Biometeorology*. **34**, pp. 98-104 (1990)

[32] Colin, J., Decharme, B., Cattiaux, J., & Saint-Martin, D. Groundwater Feedbacks on Climate Change in the CNRM Global Climate Model. *Journal of Climate*. **36**, 7599-7617 (2023) `https://doi.org/10.1175/JCLI-D-22-0767.1`

[33] Roehrig, R., Beau, I., Saint-Martin, D., Alias, A., Decharme, B., Guérémy, J.-F., et al. The CNRM global atmosphere model ARPEGE-Climat 6.3: Description and evaluation. *Journal of Advances in Modeling Earth Systems*. **12** e2020MS002075 (2020) `https://doi.org/10.1029/2020MS002075`

[34] Masson, V., Le Moigne, P., Martin, E., Faroux, S., Alias, A., Alkama, R., Belamari, S., Barbu, A., Boone, A., Bouyssel, F. & Others The SURFEXv7. 2 land and ocean surface platform for coupled or offline simulation of earth surface variables and fluxes. *Geoscientific Model Development*. **6**, 929-960 (2013)

[35] Decharme, B., Delire, C., Minvielle, M., Colin, J., Vergnes, J.-P., Alias, A., et al. Recent changes in the ISBA-CTRIP land surface system for use in the CNRM-CM6 climate model and in global off-line hydrological applications. *Journal of Advances in Modeling Earth Systems*. **11** 1207–1252 (2019) `https://doi.org/10.1029/2018MS001545`

[36] Delire, C., Séférian, R., Decharme, B., Alkama, R., Calvet, J.-C., Carrer, D., et al. The global land carbon cycle simulated with ISBA-CTRIP: Improvements over the last decade. *Journal of Advances in Modeling Earth Systems*. **12** e2019MS001886 (2020) `https://doi.org/10.1029/2019MS001886`

[37] Decharme, B., Costantini, M., Colin, J. A simple Approach to Represent Irrigation Water Withdrawals in Earth System Models *Journal of Advances in Modeling Earth Systems*. Under review (2024)